Aerosol and Air Quality Research, 17: 1837–1855, 2017

ISSN: 1680-8584 print / 2071-1409 online
doi: 10.4209/aaqr.2016.04.0151

Impacts of Upstream Building Height and Stack Location on Pollutant Dispersion from a Rooftop Stack

Yuan-Dong Huang[1*], Ye Song[1], Xuan Xu[1], Wen-Rong He[1], Chang-Nyung Kim[2,3]

[1] *School of Environment and Architecture, University of Shanghai for Science and Technology, Shanghai 200093, China*
[2] *College of Engineering, Kyung Hee University, Yongin 449-701, Korea*
[3] *Industrial Liaison Research Institute, Kyung Hee University, Yongin 449-701, Korea*

ABSTRACT

This paper presents Computational Fluid Dynamics (CFD) simulations to evaluate the impacts of the upstream building height and stack location on the dispersion of the pollutant released from a rooftop stack. The simulations are performed with the 3D, steady, Reynolds-Averaged Navier-Stokes (RANS) equations coupled with Realizable k-ε turbulence model and the species transport equation. The flow development and pollutant dispersion are investigated numerically considering four different upstream building height (H_{B1}) to emitting building height (H_{B2}) ratios (H_{B1}/H_{B2} = 0.5, 1.0, 2.0 and 3.6) and four different stack locations measured from the upwind edge of the emitting building (X_s) under the approaching wind perpendicular to the building faces. The results obtained reveal that: (1) the flow field characteristics around the buildings, especially the vortex flow above the emitting building roof and the vortex pattern between the upstream and emitting buildings, depend significantly on the upstream building height and much less on the location of the short stack; (2) for an upstream building of lower or equal height with the emitting building, the pollutants from a rooftop stack are immediately transported downwind the stack by the longitudinal flow; (3) when a stack is located inside the wake recirculation zone of the upstream building, the pollutants from the stack are swept by the upwind flow towards the leeward side of the upstream building and the distribution of pollutant concentrations is highly sensitive to both the upstream building height and the stack location. For different upstream building heights, suitable locations for fresh air intakes on the sides of buildings are also proposed based on the pollutant distribution patterns obtained.

***Keywords*:** Pollutant dispersion; Airflow; Rooftop stack; Upstream building; Numerical simulation.

INTRODUCTION

The study on dispersion of gaseous pollutants released from rooftop stacks in urban environment has gained great concern during the past two decades due to the potential health hazards associated with rooftop stack emissions. Because of the complex wind field around buildings, pollutants discharged from a building roof may get re-entrained into the same building or enter into the surrounding buildings leading to poor indoor air quality in these buildings (Wilson *et al.*, 1998; Hajra *et al.*, 2011; Gupta *et al.*, 2012).

Previous studies have revealed that the dispersion of pollutants released from rooftop stacks is influenced greatly by many factors, such as the ambient wind conditions (atmospheric stability, wind direction and wind speed), stack conditions (size and location of a stack, and stack exhaust momentum), rooftop structures (RTSs) and building configurations. For instance Yassin (2013) performed wind tunnel experiments to examine the effects of stack location and atmospheric stability on the airflow and dispersion of the pollutants emitted from a stack positioned on the roof of an isolated building by considering the three different atmospheric stabilities (stable, neutral and unstable) and three stack locations. The results show that the vertical distributions of wind velocity and concentration in the near wake of the emitting building are affected significantly by both the stack location and atmospheric thermal stability. Gupta *et al.* (2012) conducted a wind tunnel investigation of the downwash effect caused by a RTS on the dispersion of pollutants emitted from a short stack placed on an isolated building roof. The results reveal that the roof level concentrations are increased greatly by the presence of RTS depending on the building height, wind direction, stack condition (exhaust speed, location and height) and RTS crosswind width. Hajra *et al.* (2012) performed a wind tunnel study to assess the effect of downstream buildings on the dispersion of effluents from a rooftop stack. In the wind tunnel simulations, nine different building configurations,

* Corresponding author.
Tel.: +86-021-55275611; Fax: +86-021-55275979
E-mail address: huangyuandong@tsinghua.org.cn

three exhaust momentum ratios and three stack heights were taken into account for wind orthogonal to the building faces. The results show that the dispersion process of the effluents is affected greatly by the height and across-wind-dimension of the downstream building, as well as the spacing between the emitting and downstream buildings.

Recently, Hajra *et al.* (2011) conducted an intensive wind tunnel study to evaluate the effect of upstream buildings on the pollutant dispersion from rooftop stacks in the built environment. The wind tunnel tests were performed for nine different building configurations under three exhaust momentum ratios, three stack heights, two stack locations, and three spacing between the two buildings. Pollutant concentrations were measured on the roof and leeward wall of the emitting and upstream buildings. The experimental data show that when the stack is located within the recirculation zone of the upstream building, the dilution of emissions from the downwind building is affected greatly by the upstream building height and the spacing between the two buildings and much less affected by the along-wind-dimension of the upstream building. In the wind tunnel experiments of Hajra *et al.* (2011), three different upstream building heights and two different stack locations were considered. However, the pollutant concentrations were only measured along the building centerline and, not laterally over the various building surfaces (i.e., the pollutant concentration fields were not obtained in the experiments). On the other hand, the stack was only located upwind the center of the emitting building roof, and the effect of the stack location downwind the center of the emitting building roof was not taken into consideration. Furthermore, the wind flow field around the buildings which governs the pollutant dispersion patterns was not measured in the experiments. Chavez *et al.* (2012) carried out a CFD study to assess the effect of upstream buildings on the pollutant dispersion from a rooftop stack. The numerical results show that when the pollutant source is located within the wake zone behind the upstream building, the pollutant dilution is highly sensitive to the height of the upstream building and much less sensitive to its width and length. In the CFD simulations of Chavez *et al.* (2012), six different upstream building heights (H_{B1}/H_{B2} = 1.0, 1.33, 1.7, 2.0, 2.8 and 3.6) were utilized. However, the stack was only located in the center of the emitting building roof for each of the above six upstream building heights. Obviously, although the changes of upstream building heights and stack locations were taken into account in the previous studies on the near-field pollutant dispersion from rooftop stacks, further research work is still needed in order to clarify systematically the effects of upstream building height under various stack locations (i.e., the combined effects of upstream building height with stack location) on the airflow around buildings and the dispersion pattern of pollutants released from rooftop stacks.

This paper presents three-dimensional Computational Fluid Dynamics (CFD) simulations to evaluate the combined effects of upstream building height and stack location on the dispersion of gaseous pollutants emitted from a rooftop stack. The simulations are performed using the steady Reynolds-Averaged Navier-Stokes (RANS) equations coupled with the Realizable k-ε turbulence model and the inert species transport equation. In the CFD modeling, the approaching wind is orthogonal to the building faces and the pollutants (SF_6 in the current study) are released from a short stack on the emitting building roof. The flow development and pollutant dispersion are investigated numerically taking into account four different upstream building heights as well as four different stack locations measured from the upwind edge of the emitting building. The streamlines and normalized dilution contours on the middle vertical plane passing through the center of the stack outlet, the horizontal plane at the stack height and the horizontal plane at the human respiration height for four different upstream building heights under each of the four stack locations are obtained, which are analyzed comprehensively to explore the influences of both the upstream building height and stack location on the dilution of pollutants released from a rooftop stack. Furthermore, suitable locations for fresh air intakes on the sides of buildings under different upstream building heights are also proposed based on the pollutant distribution patterns obtained.

METHODOLOGY

Physical Model Setup

In the present study, the physical model configurations are constructed based on the wind tunnel models adopted in the wind tunnel experiments carried out by Chavez *et al.* (2012) at the Boundary Layer Wind Tunnel of Concordia University.

Fig. 1 illustrates the schematic sketches of the physical model configurations under study. In each configuration, the dimensions of the emitting building named B2 are 0.25 (length) × 0.25 (width) × 0.075 (height) m^3 (a reduced scale model with scale 1:200 is employed in the present work), whereas the building called B1 which is positioned upstream of B2 is 0.075 m long and 0.25 m wide. Fixed spacing of 0.1 m between B1 and B2 is applied to all configurations. Tracer gas consisting of a mixture of Sulfur hexafluoride (SF_6, pollutant) and Nitrogen is released from a stack located centrally on the rooftop of B2 (the stack location is 0.125 m from the lateral edges of B2). In each configuration the stack is set as 0.005 m high, with an internal diameter of 0.003 m. For evaluating the influence of upstream building height (H_{B1}) on airflow and pollutant dispersion from the rooftop stack, four different heights of the upstream building (i.e., H_{B1}= 0.0375, 0.075, 0.15 and 0.27 m, respectively) are considered. For investigating the effect of stack location on pollutant dispersion, four different distances X_s from the stack to the upwind edge of building B2 (i.e., X_s = 0.05, 0.1, 0.15 and 0.2 m, respectively) are assumed for each of the above four upstream building heights. Therefore, sixteen physical model configurations are generated by the combinations of the four upstream building heights and four stack locations, which are listed in Table 1.

In each case, the approaching wind (i.e., the undisturbed airflow) is perpendicular to the windward face of B1 and has a velocity of 6.2 m s^{-1} at the B2 height (detailed velocity boundary condition is to be given later). For all cases the

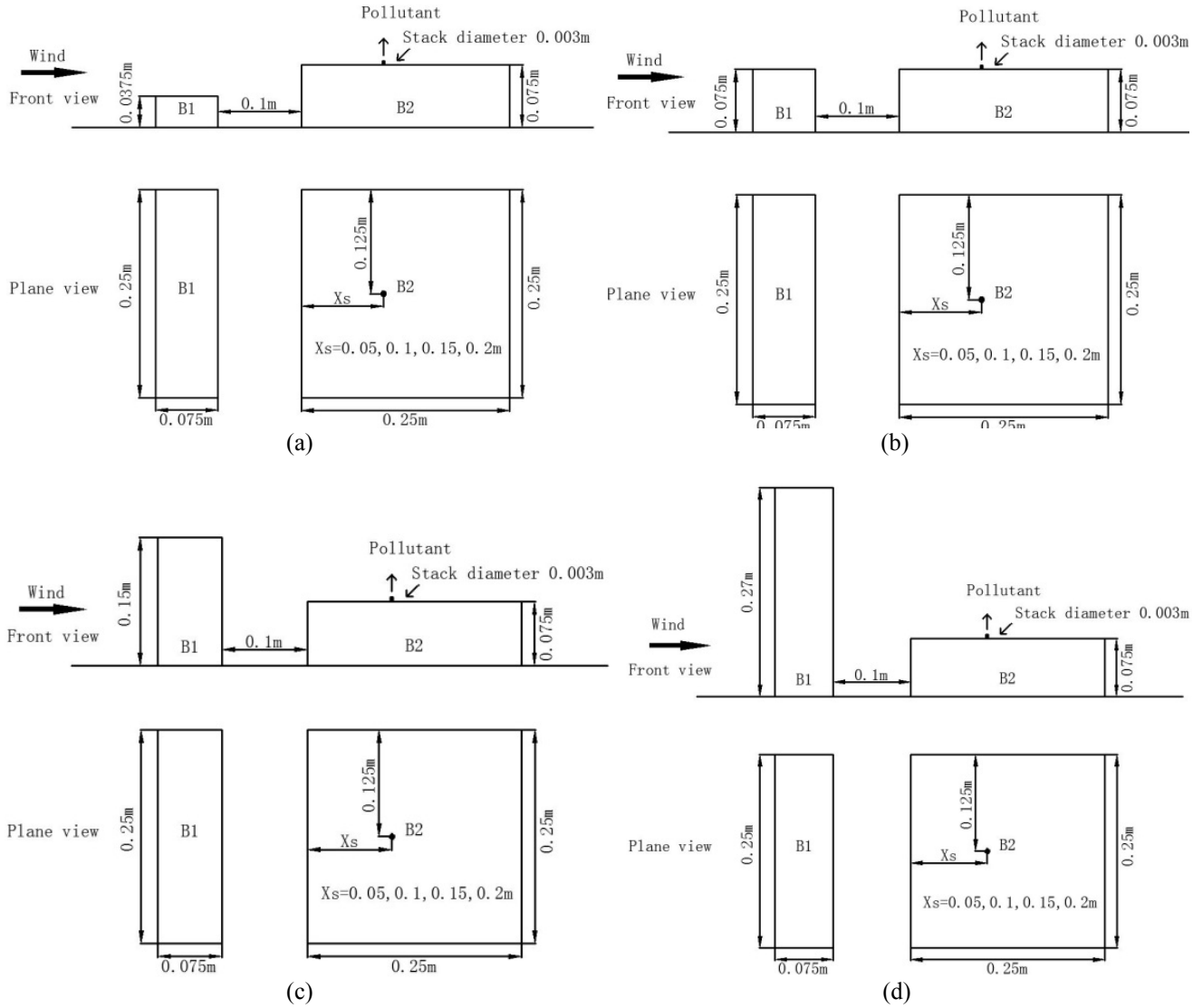

Fig. 1. Schematic sketches of the physical model configurations. (a) Cases with H_{B1} = 0.0375 m, (b) Cases with H_{B1} = 0.075 m, (c) Cases with H_{B1} = 0.15 m and (d) Cases with H_{B1} = 0.27 m.

Table 1. Cases considered.

		X_s			
		0.05 m	0.1 m	0.15 m	0.2 m
H_{B1}	0.0375 m	Case 1	Case 2	Case 3	Case 4
	0.075 m	Case 5	Case 6	Case 7	Case 8
	0.15 m	Case 9	Case 10	Case 11	Case 12
	0.27 m	Case 13	Case 14	Case 15	Case 16

exhaust velocity at the stack is 6.2 m s^{-1} (i.e., the momentum ratio at the stack outflow is $M = V_e/U_{B2} = 1$, where V_e is the exhaust velocity and U_{B2} the approaching wind speed at the B2 height) and the concentration of SF_6 in the mixture emitted from the stack is 10 ppm.

CFD Model

In this study, the numerical model for simulating airflow and pollutant dispersion is established and solved, using the commercial CFD code ANSYS FLUENT.

Governing Equations for Airflow and Pollutant Dispersion

For the turbulent wind flow around buildings, as depicted in Fig. 1, the equations governing the flow field consist of the continuity equation and the RANS equations. Different turbulence models have been adopted in the simulations of airflow past bluff bodies (Tominaga and Stathopoulos, 2009; Ramponi and Blocken 2012). However, the optimum choice of turbulence model is still not available in the literature. The reason is that turbulence models' performance depends on different situations (Chavez *et al.* 2012). This

work uses the Realizable k-ε turbulence model, based on the previous research performed by Chavez *et al.* (2011, 2012).

For the simulation of pollutant dispersion, the steady species (pollutants) transport equation is applied (Huang *et al.* 2014), giving

$$u_j \frac{\partial C^\alpha}{\partial x_j} = \frac{\partial}{\partial x_j}\left(\left(D_m^\alpha + \frac{\nu_t}{Sc_t}\right)\frac{\partial C^\alpha}{\partial x_j}\right) \quad (1)$$

where u_j is the mean velocity component in Cartesian coordinate x_j (j = 1, 2, 3), C^α is the concentration of chemical species α, D_m^α is the molecular diffusivity for species α in the mixture, ν_t is the turbulent eddy viscosity, and Sc_t (= 0.7, a default value in FLUENT) is the turbulent Schmidt number.

Computational Domain and *Boundary Conditions*

Fig. 2 shows the computational domain for the Cases 9-16 (i.e., the cases with $H_{B1} > H_{B2}$, where H_{B2} is the height of the emitting building). Here, the inlet plane is $3H_{B1}$ away from the upstream building and the outlet plane is $20H_{B1}$ downwind from the emitting building to allow full development of the flow; the lateral and the top boundaries are $5H_{B1}$ away from the upstream building. Thus, the computational domain is 3.875 m long × 1.75 m wide × 0.9 m high for each of the Cases 9–12 while it is 6.635 m long × 2.95 m wide × 1.62 m high for each of the Cases 13–16. For each of the Cases 1–8 (i.e., the cases with $H_{B1} \le H_{B2}$), the computational domain is the same as that for each of the Cases 9–12.

The approaching wind velocity and turbulence intensity profiles measured in the wind tunnel experiment of Chavez *et al.* (2012) (see Fig. 3) are used to specify the inlet boundary condition. Here, the inlet mean wind speed can be approximately described by the following power law profile:

$$U(z) = 6.2\left(\frac{z}{0.075}\right)^{0.31} \text{ m s}^{-1} \quad (2)$$

where $U(z)$ is the average wind speed at the height z above the ground.

The turbulent kinetic energy and dissipation rate profiles at the inlet boundary are specified as follows:

$$k = 0.5(TI(z)U(z))^2 \quad (3)$$

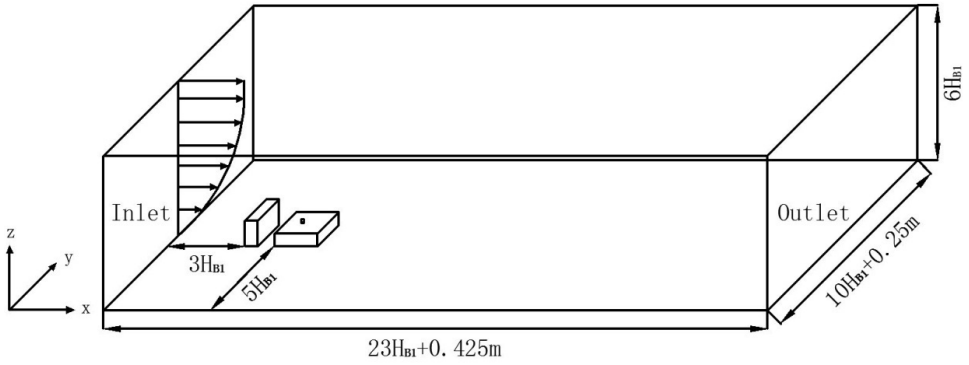

Fig. 2. Computational domain for the Cases with $H_{B1} > H_{B2}$.

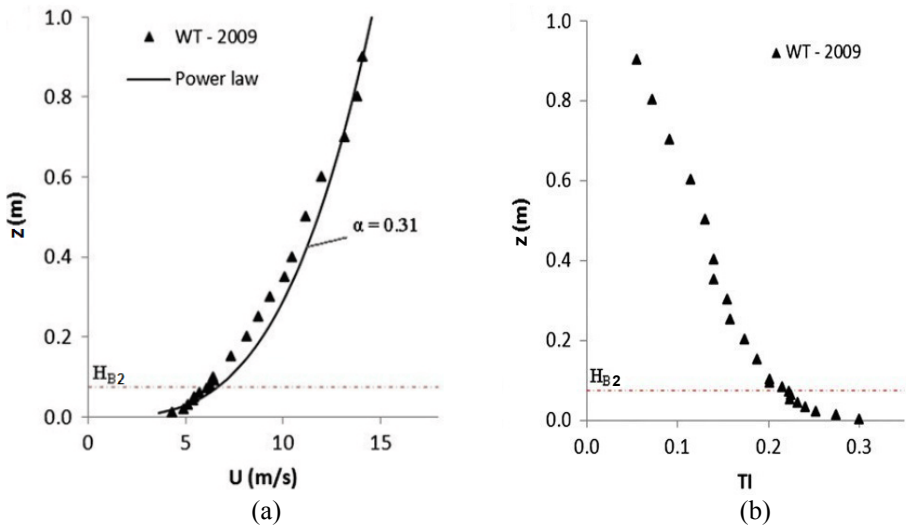

(a) (b)

Fig. 3. Inlet profile measurements from the wind tunnel experiment. (a) Mean velocity profile and (b) turbulence intensity (Chavez *et al.*, 2012).

$$\varepsilon = \frac{u_*^3}{\kappa z} \tag{4}$$

where k is the turbulent kinetic energy, $TI(z)$ is the turbulent intensity at the height z, ε is the turbulent dissipation rate and κ is the von Karman constant (0.4). u_* is the friction velocity, which is obtained from the following equation:

$$\frac{U(z)}{u_*} = \frac{1}{\kappa}\ln\left(\frac{z}{z_0}\right) \tag{5}$$

where z_0 = 0.0033 m is the roughness length.

At the inlet boundary, the pollutant concentrations are set to zero (free of pollutants).

At the outlet boundary, an outflow (zero-gradient) condition is applied to produce a fully developed flow. At the top and lateral sides of the domain, a symmetry condition is assumed. On all the solid surfaces, non-slip conditions are imposed.

The pollutant released from the rooftop stack is simulated with SF_6 for $Q = 4.38 \times 10^{-5}$ m^3 s^{-1} (Q is the flow rate of the mixture at the stack outlet) and C_e = 10 ppm (C_e is the concentration of SF_6 in the exhaust).

Grids and Numerical Scheme

The computational domain is discretized using tetrahedral grids. The smallest grid cells near the building surfaces and around the stack have an edge length of 0.001 m. The grid cells are expanded from the building wall surfaces, roofs and the stack surface towards the inlet, outlet, lateral and top boundaries of the domain. The expansion ratio between two consecutive cells is limited to 1.05 and the largest grid cell has an edge length of 0.0035 m. Thus, the total number of grid cells is about 2.5×10^6 for each of the Cases 1–12, and 3.7×10^6 for each of the Cases 13–16.

The numerical simulations are performed with the ANSYS FLUENT code. The SIMPLE algorithm is utilized for the pressure-velocity coupling. The second-order upwind discretization schemes are employed for all the transport equations (momentum, turbulent kinetic energy, turbulent dissipation rate and species concentration). During the process of calculation, the maximum iteration step is set at 4000 and the convergence criterion for all non-dimensional residuals is fixed at 10^{-6}.

RESULTS AND DISCUSSION

In this study, the dispersion of the pollutant from a rooftop stack is evaluated in terms of the normalized dilution (Chavez *et al.*, 2011):

$$D_{normalized} = \frac{D_r Q}{U_{B2} H_{B2}^2} \tag{6}$$

where $D_r = C_e/C_r$ is the dilution at a coordinate location, with C_r the pollutant concentration at the corresponding location (ppm). In the current study, C_e = 10 ppm, $Q = 4.38 \times 10^{-5}$ m^3 s^{-1}, U_{B2} = 6.2 m s^{-1} and H_{B2} = 0.075 m, so that $D_{normalized} = 1.256 \times 10^{-8}/C_r$. Obviously, at a given coordinate location the pollutant concentration is inversely proportional to the normalized dilution.

It should be noted that although D_r is expressed as C_e/C_r, the concentration at a coordinate location, C_r is proportional to the pollutant emission rate and not the pollutant concentration at emission, C_e (Hajra *et al.*, 2011). In the present study, the normalized dilution ($D_{normalized}$) instead of the dilution (C_r) is used, since the normalized dilution takes the effects of pollutant emission rate and approaching wind speed on pollutant dispersion from a rooftop stack into account. Moreover, the normalized dilution is adopted in this study in purpose of comparison with previous studies of Chavez *et al.* (2012) (the normalized dilution was adopted in a CFD study conducted by Chavez *et al.* (2012) to evaluate the effect of upstream buildings on the pollutant dispersion from a rooftop stack).

Effects of the Upstream Building of Lower or Equal Height with the Emitting Building

Fig. 4 shows the streamlines and normalized dilution contours on the middle vertical plane (this vertical plane passes through the center of the stack outlet) and on the horizontal plane at the stack height (z = 0.08 m) for four different stack locations under an upstream building height of 0.0375 m (H_{B1}/H_{B2} = 0.5) (since only the mean flow is simulated for each case, a half horizontal plane located at the stack height is selected in consideration that the mean airflow is symmetrical with respect to the middle vertical plane). In Fig. 4, the streamline patterns on the vertical plane clearly indicate that a large clockwise vortex between the two buildings and a large wake vortex zone behind the emitting building are produced for each of the Cases 1–4. These streamlines on the vertical plane also show that a minor recirculation zone is developed just behind the stack for cases with X_s = 0.05 and 0.1 m, while this small vortex zone behind the stack is merged into the large wake vortex zone behind the emitting building for cases with X_s = 0.15 and 0.2 m. Furthermore, the streamline patterns on the horizontal plane reveal that the wind flows along almost the approaching wind direction on the horizontal plane at the stack height (i.e., the cross flow is not set up) for each of the Cases 1–4.

It is well known that pollutant dispersion within an urban environment is dominated by the turbulent airflow pattern (Li *et al.*, 2006). In Fig. 4, the normalized dilution contours on both the vertical and horizontal planes show that high pollution levels are formed on the emitting building roof downwind the stack and in the wake recirculation zone behind the emitting building, while the region upwind the stack is free of pollutants, for each of the Cases 1–4. This is because the pollutants emitted from the rooftop stack are directly conveyed downstream by the turbulent flow moving almost in the direction parallel with the approaching wind enhancing the dilution of pollutants by mixing the pollutants with the atmospheric clean air. The normalized dilution contours in Fig. 4 also show clearly that the polluted zone on the emitting building roof is diminished as the stack moves closer to the downwind edge of the emitting building.

Fig. 5 presents the streamlines and normalized dilution field on the middle vertical plane and on the horizontal plane located at the stack height at four different stack locations for an upstream building height of 0.075 m (H_{B1}/H_{B2} = 1.0). The figure illustrates clearly that a tiny recirculation zone near the ground next to the windward wall of the upstream building (not observed in the Cases 1–4), a small recirculation zone above the upstream building roof (not observed

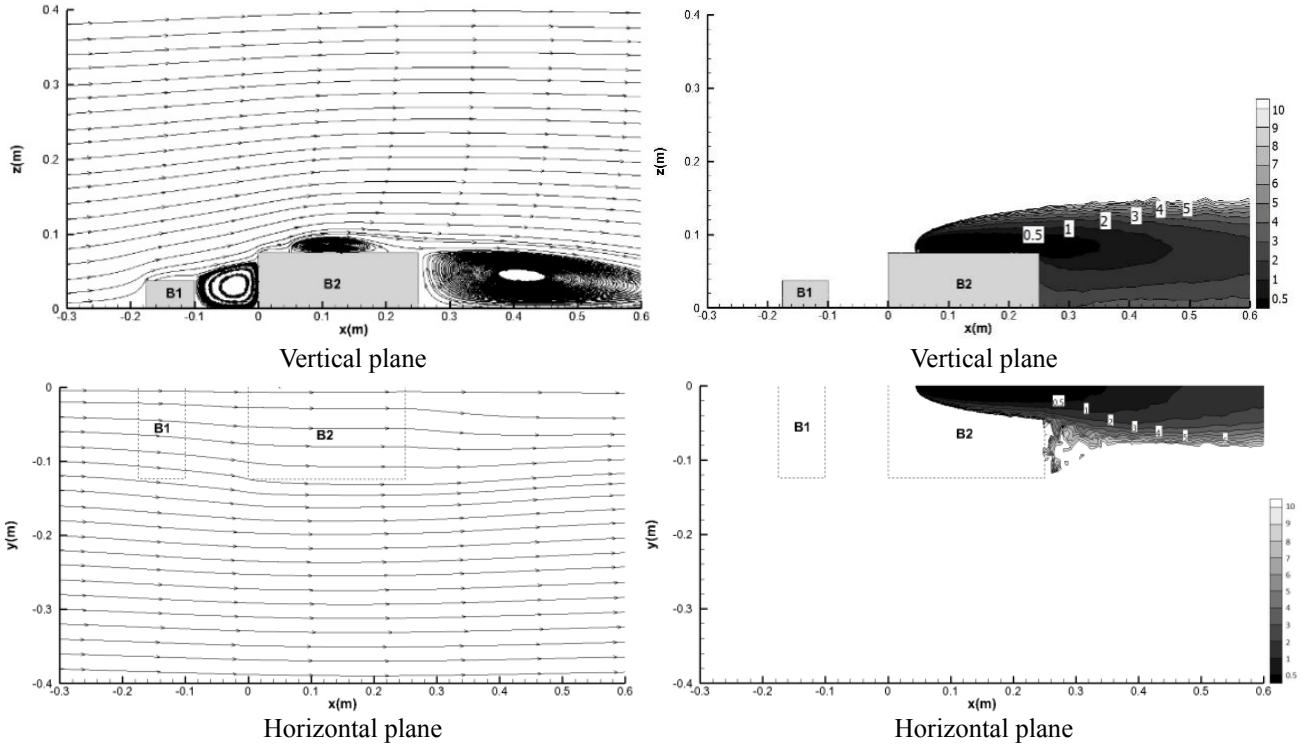

(a) Case 1 (H_{B1} = 0.0375 m, X_s = 0.05 m)

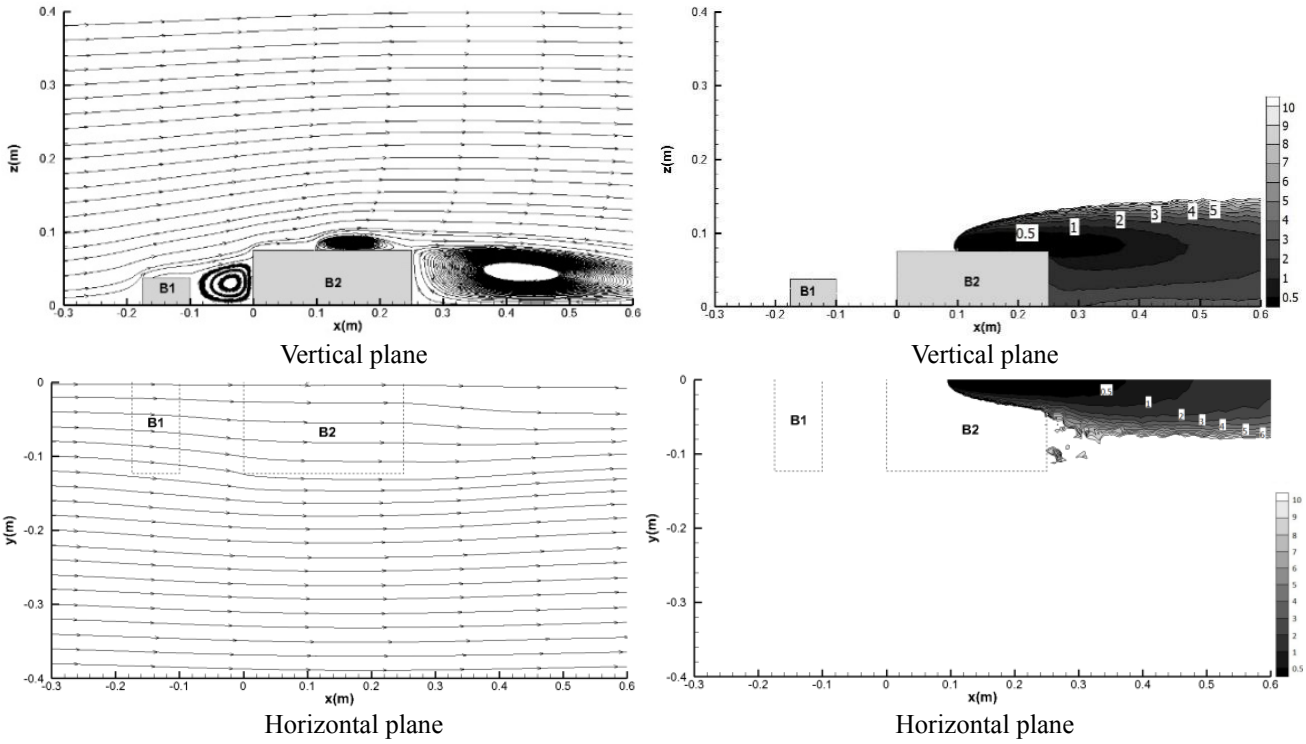

(b) Case 2 (H_{B1} = 0.0375 m, X_s = 0.1 m)

Fig. 4. Streamlines and normalized dilution contours on the middle vertical plane and on the half horizontal plane at the stack height (z = 0.08 m) for the Cases 1–4 (H_{B1} = 0.0375 m, X_s = 0.05, 0.1, 0.15, 0.2 m).

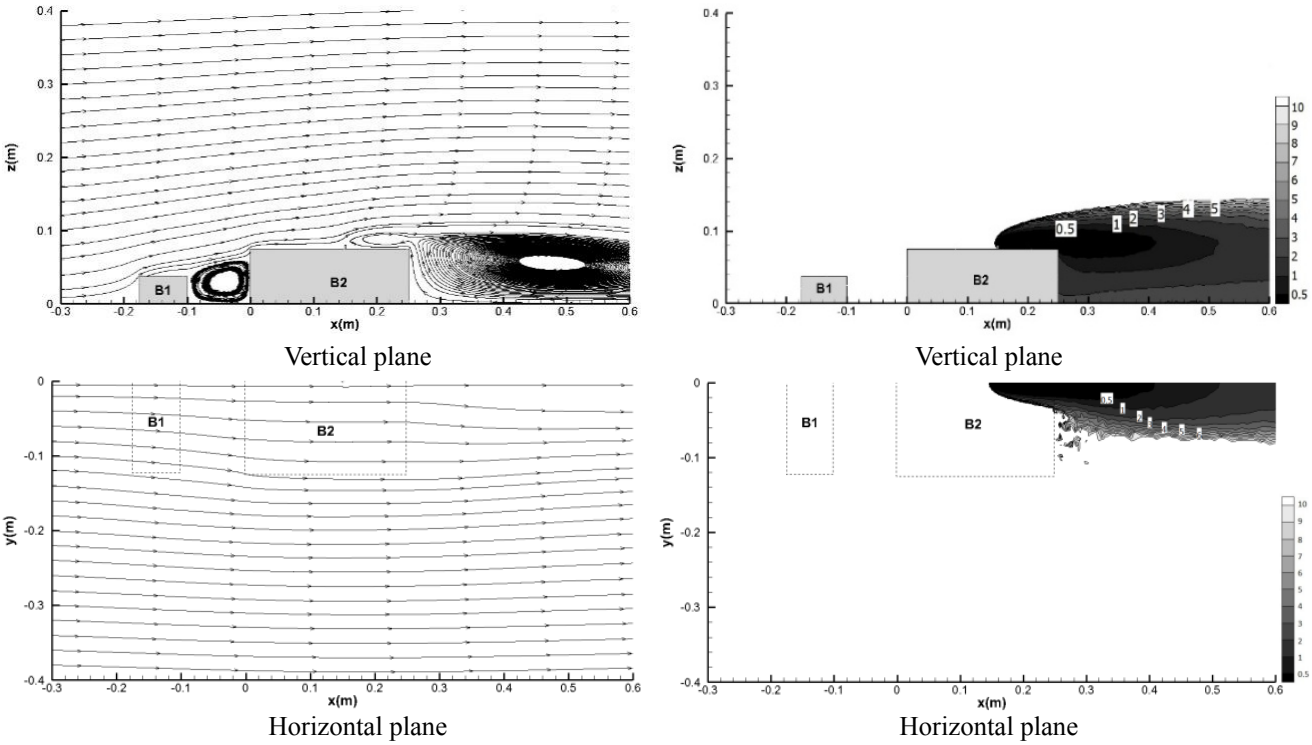

Vertical plane Vertical plane

Horizontal plane Horizontal plane

(c) Case 3 (H_{B1} = 0.0375 m, X_s = 0.15 m)

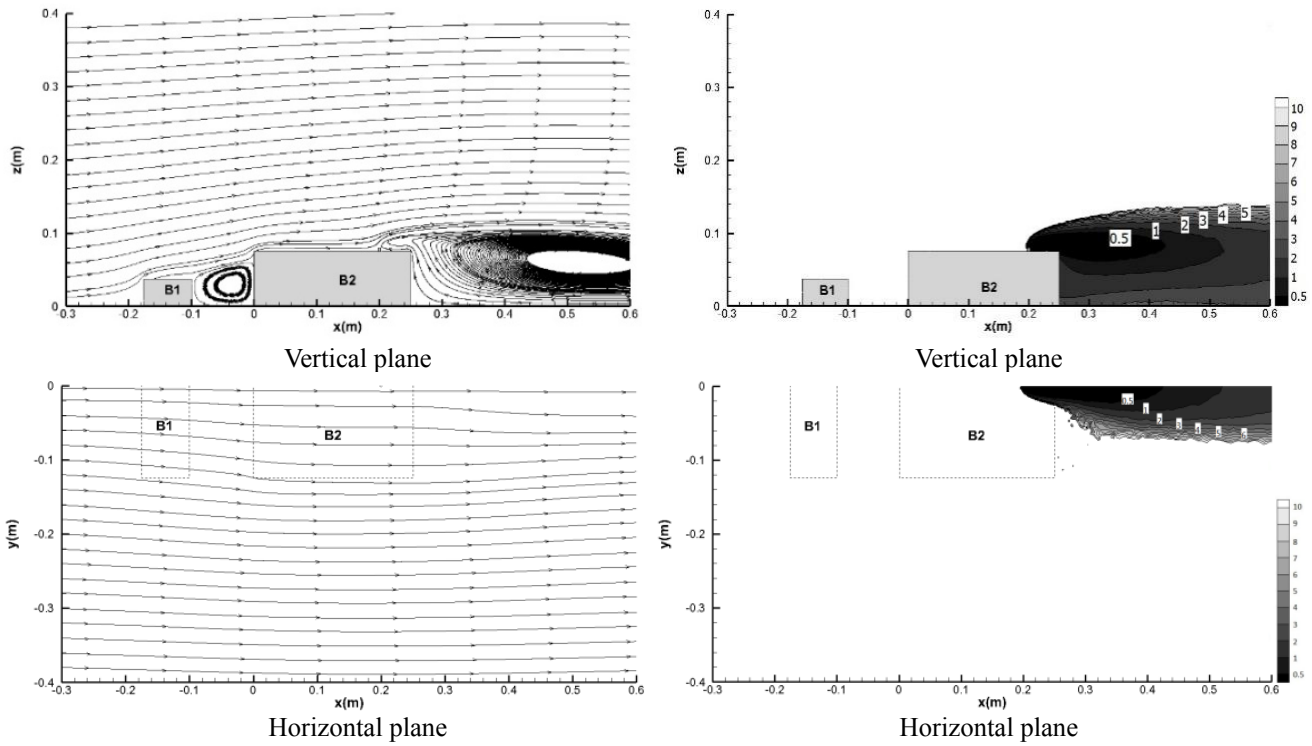

Vertical plane Vertical plane

Horizontal plane Horizontal plane

(d) Case 4 (H_{B1} = 0.0375 m, X_s = 0.2 m)

Fig. 4. (*continued*).

obviously in the Cases 1–4), a well-organized clockwise vortex placed between the two buildings and a large wake vortex zone behind the emitting building are established in the middle vertical plane for each of the Cases 5–8. Comparing Fig. 5 with Fig. 4, it is evident that on the middle vertical plane the clockwise vortex between the two buildings for the Cases 5–8 is larger significantly than that for the Cases 1–4, whereas the wake zone behind the emitting building for the Cases 5–8 is smaller than that for the Cases 1–4. Fig. 5 also shows clearly that there is no cross flow formed

on the horizontal plane at the stack height for each of the Cases 5–8 (these flow patterns are very similar to those observed in the Cases 1–4). Furthermore, it is revealed from the streamlines on both the vertical and horizontal planes displayed in Fig. 5 that the general flow field is almost unaffected by the existence of the stack under the condition of $H_{B1} = H_{B2} = 0.075$ m.

In Fig. 5, the normalized dilution fields on both the

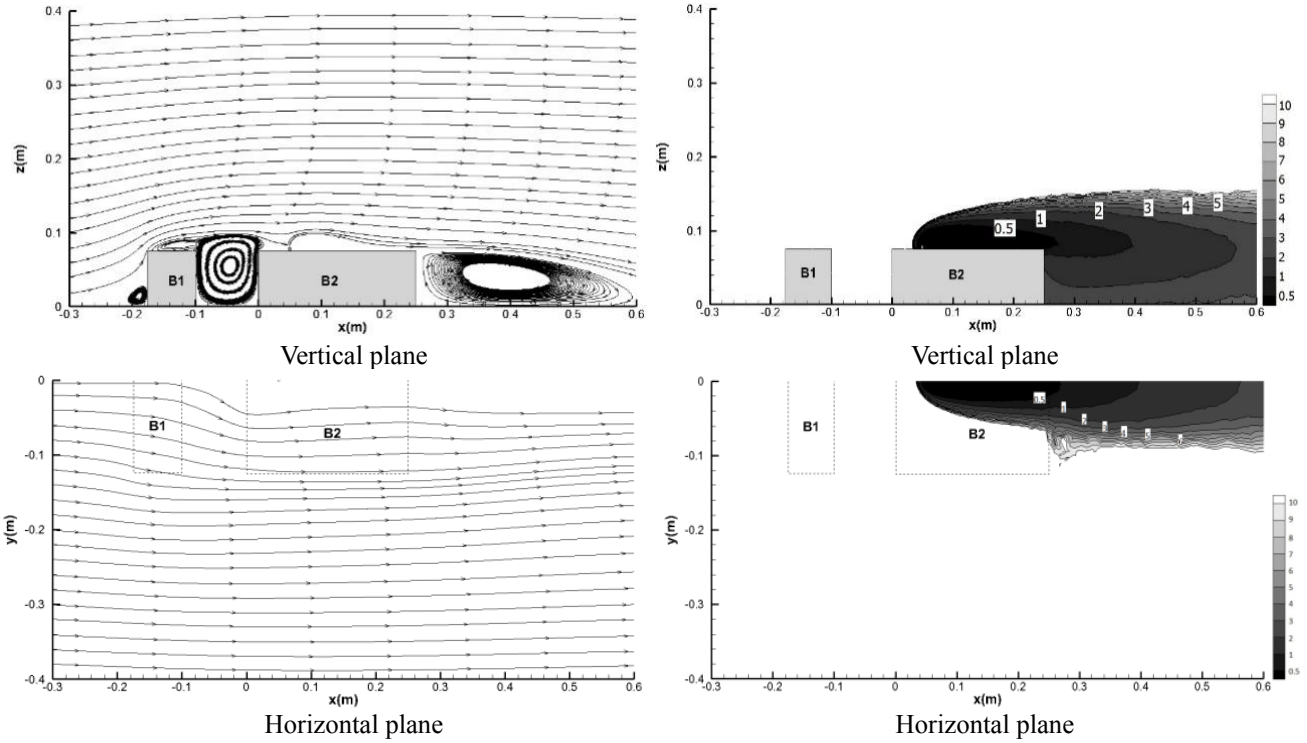

Vertical plane Vertical plane

Horizontal plane Horizontal plane

(a) Case 5 (H_{B1} = 0.075 m, X_s = 0.05 m)

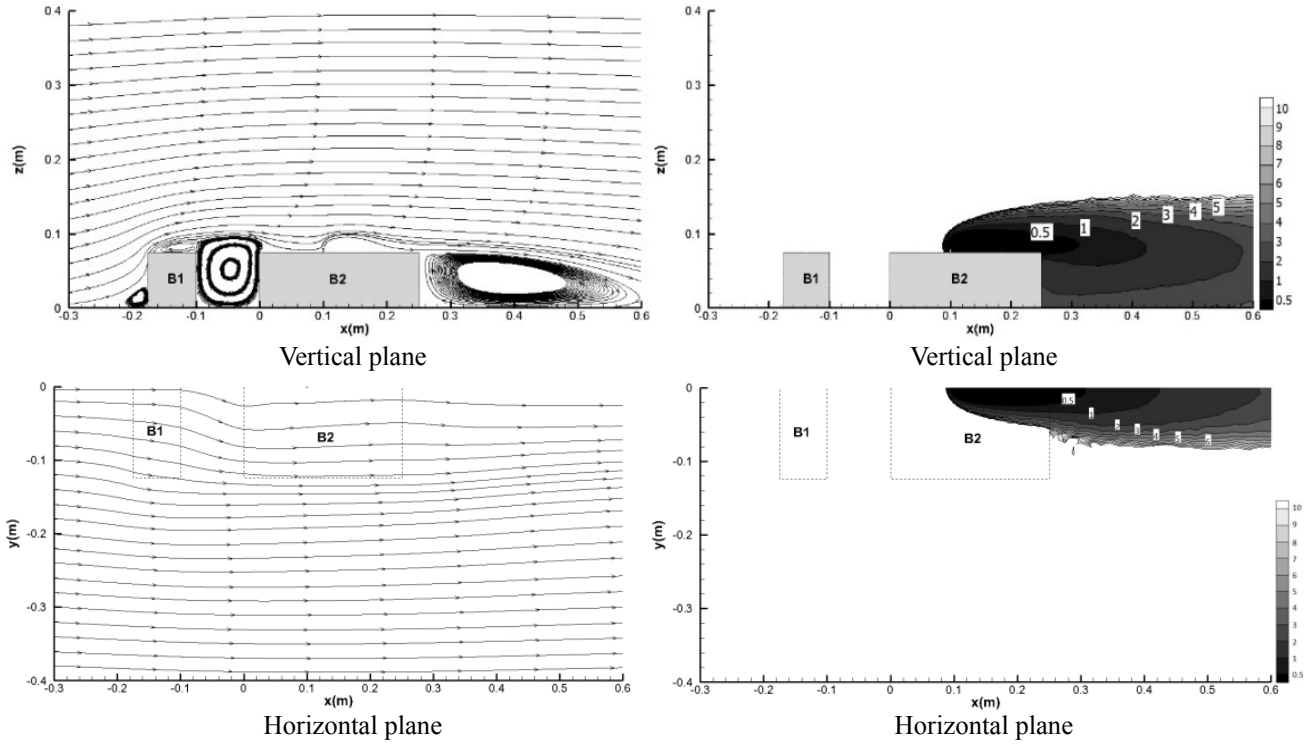

Vertical plane Vertical plane

Horizontal plane Horizontal plane

(b) Case 6 (H_{B1} = 0.075 m, X_s = 0.1 m)

Fig. 5. Streamlines and normalized dilution contours on the middle vertical plane and on the half horizontal plane at the stack height (z = 0.08 m) for the Cases 5–8 (H_{B1} = 0.075 m, X_s = 0.05, 0.1, 0.15, 0.2 m).

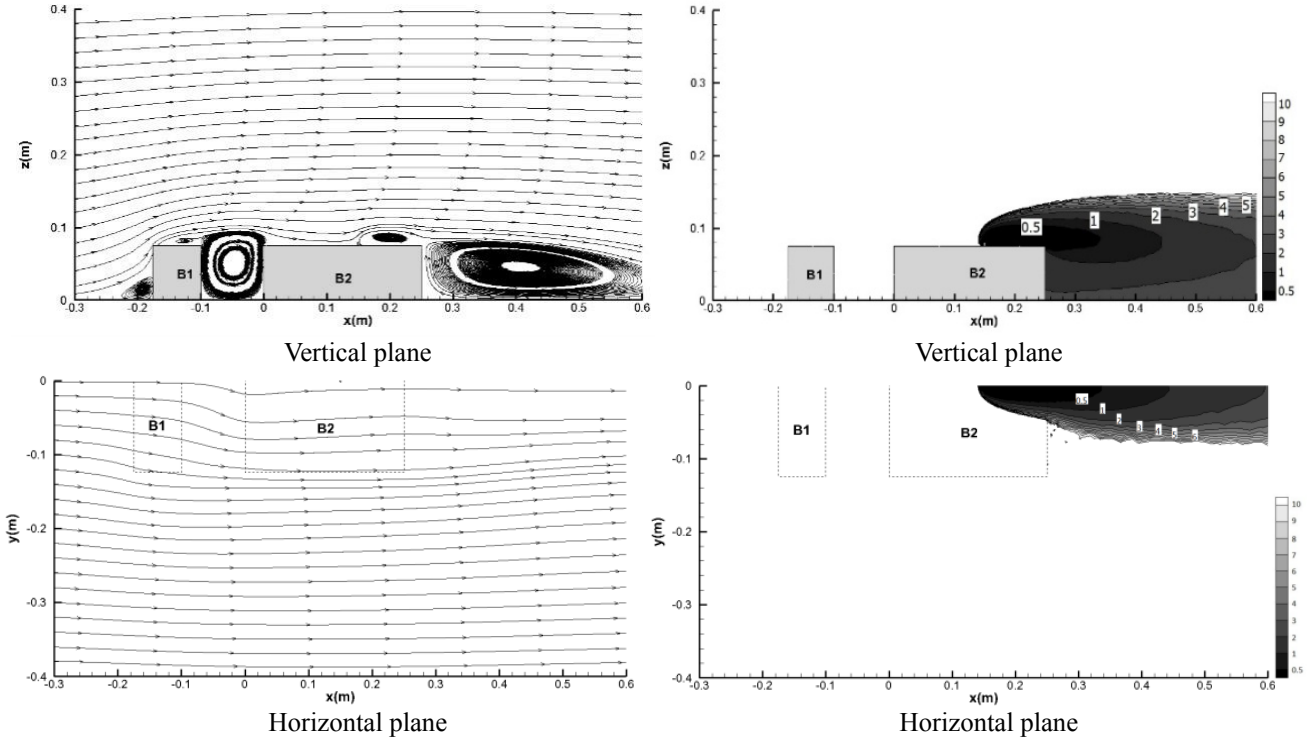

Vertical plane Vertical plane

Horizontal plane Horizontal plane

(c) Case 7 (H_{B1} = 0.075 m, X_s = 0.15 m)

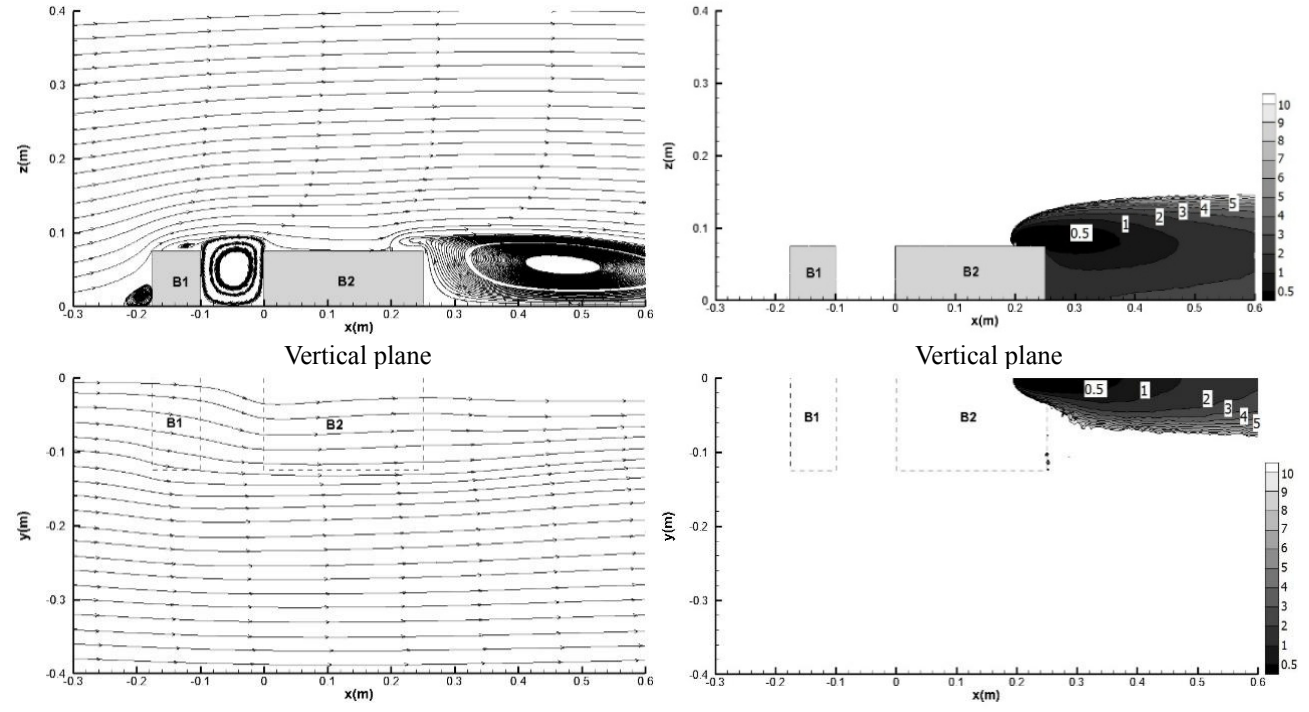

Vertical plane Vertical plane

Horizontal plane Horizontal plane

(d) Case 8 (H_{B1} = 0.075 m, X_s = 0.2 m)

Fig. 5. (*continued*).

vertical and horizontal planes show that the pollutants are distributed on the emitting building roof downwind the stack and in the wake recirculation zone behind the emitting building (as previously observed in the Cases with H_{B1} = 0.0375 m). This is also because the pollutants emitted from the rooftop stack are immediately transported downstream by the airflow moving almost in the direction parallel with the approaching wind for the Cases 5–8. The normalized dilution fields in Fig. 5 also shows clearly that the polluted area formed on the emitting building roof decreases with

an increase of the distance between the stack and the upwind edge of the emitting building (X_s). It should be noted that on the horizontal plane at the stack height the pollutant distribution along the building width direction is established mainly by the turbulent dispersion for each of the Cases 1–8 (because the mean cross flow is not developed on the horizontal plane at the stack height). Comparing Fig. 5 with Fig. 4, it is obvious that for a given stack location (especially, for X_s = 0.05 and 0.1 m) the polluted zone on the horizontal plane at the stack height is wider at H_{B1} = 0.075 m than that at H_{B1} = 0.0375 m.

Based on the above pollutant distribution characteristics in the Cases 1–8, it is clear that for the case with an upstream building of lower or equal height with the emitting building fresh air intakes should not be placed on the emitting building roof downwind the stack or on the leeward wall of the emitting building. Instead, the intakes can be located on the whole upstream building surfaces, on the lateral and windward walls of the emitting building, and on the emitting building roof upwind the stack.

Effects of the Upstream Building Higher than the Emitting Building

Fig. 6 presents the streamlines and normalized dilution fields on the middle vertical plane and on the horizontal plane at the stack height for four different stack locations with an upstream building height of 0.15 m (H_{B1}/H_{B2} = 2.0). These streamlines on the vertical and horizontal planes reveal clearly that the turbulent flow pattern is almost identical in each of the Cases 9–12 (i.e., the impact of stack location on the general flow pattern is negligible since the stack is very smaller than the two buildings). The streamlines on the middle vertical plane show a combination of upwind and downwind flow above the roof surface of building B2 (the turning point between the upwind and downwind flow is near to the downwind edge of B2). This is because the emitting building is only partly located within the wake region of the upstream building, causing that the air above the B2 roof placed inside the wake zone of B1 flows upwind whereas the air above the B2 roof positioned outside the wake zone of B1 moves downwind. The streamlines on the vertical plane also show that a counter-clockwise vortex between the two buildings is established due to the strong induction of the upwind flow above the B2 roof. Furthermore, the streamlines on the vertical plane show a near-ground clockwise vortex next to the windward wall of B1 and a wake recirculation zone behind B2. Clearly, the wake recirculation zone behind B2 in each of the Cases 9–12 is significantly smaller than that in each of the Cases 5–8, while the near-ground vortex next to the windward wall of B1 in each of the Cases 9–12 is much larger than that in each of the Cases 5–8 (see a comparison of Fig. 6 with Fig. 5). The streamlines on the horizontal plane at the stack height show the important cross flow from the side (which is not observed in the Cases 1–8). Obviously, this cross flow is developed due to the flow separation as the wind flows over the sidewalls of the upstream building.

Fig. 7 shows the horizontal wind velocity component (U_x) profile along the vertical line above the stack (this vertical line passes through the central point of stack outlet) for the Cases 9–12. It should be noted here that the leftward horizontal wind velocity is negative while the rightward one is positive. Clearly, the horizontal wind velocity component immediately above the stack is directed upwind for each of the Cases 9–12. As the distance from the stack to the upwind edge of emitting building increases, the U_x directed upwind above the stack becomes weak (the maximum absolute value of U_x is 2.71 m s^{-1} for X_s = 0.05 m, 1.94 m s^{-1} for X_s = 0.1 m, 0.99 m s^{-1} for X_s = 0.15 m, and 0.32 m s^{-1} for X_s = 0.2 m, respectively) and the zone above the stack where U_x is directed upwind is diminished (the height of the zone above the stack is 0.149 m for X_s = 0.05 m, 0.142 m for X_s = 0.1 m, 0.127 m for X_s = 0.15 m, and 0.099 m for X_s = 0.2 m, respectively), suggesting that the upwind flow immediately above the stack is weakened with the increase of X_s under the condition of H_{B1}/H_{B2} = 2.0.

In Case 9, the stack is entirely located in the wake zone of B1. The normalized dilution field on the middle vertical plane for Case 9 (Fig. 6(a)) shows that the stack exhaust is dragged by the upwind flow towards the upstream building. A part of the pollutants carried by the upwind flow are trapped by the anti-clockwise vortex located between the two buildings, resulting in pollutant accumulation within the canyon enclosed by the two buildings. When the pollutants reach the leeward side of B1, they are conveyed downstream by the downwind flow (the upwind flow is immediately changed into downwind flow as the upwind flow strikes the leeward wall of B1) following a long pollutant distribution along the middle axis. The dilution field on the horizontal plane for Case 9 shows a significant pollutant distribution along the building width direction (i.e., in the y direction). This is because a part of the pollutants carried by the upwind flow are transported transversally by the cross flow.

For each of the Cases 10–11, the stack is also entirely located within the wake zone of B1. Thus, the pollutant distribution pattern in each of the Cases 10–11 is very similar to that in Case 9 (see comparisons of Fig. 6(a) with Fig. 6(b), and Fig. 6(a) with Fig. 6(c)).

In Case 12, the stack is located very near to the turning point between the upwind and downwind flow above the B2 roof. The normalized dilution field on the vertical plane for Case 12 (Fig. 6(d)) shows that most part of the pollutants released from the stack are transported directly by the downwind flow towards the region downstream the stack while only a small part of the pollutants are carried by the upwind flow towards the upstream building. The normalized dilution field on the horizontal plane at the stack height for Case 12 shows that the pollutant distribution along the building width direction is weak because only a small part of the pollutants released from the rooftop stack are swept towards the upstream building.

From Fig. 6, it can be observed clearly that the pollution levels inside the canyon and on the leeward wall of the upstream building as well as the polluted area on the horizontal plane at the stack height decrease with an increase of the distance from the stack to the upwind edge of emitting building.

From a health point of view, we should pay much attention to the pollution level at the human respiration height. Fig. 8 shows the distributions of normalized dilution contours at the height of 0.075m (corresponding to 1.5m in full scale) above the ground floor for the Cases 9–12. From Fig. 8, it is clear that the pollution level in the region between the two buildings decreases significantly with an increase of X_s while the pollution level in the wake region behind the

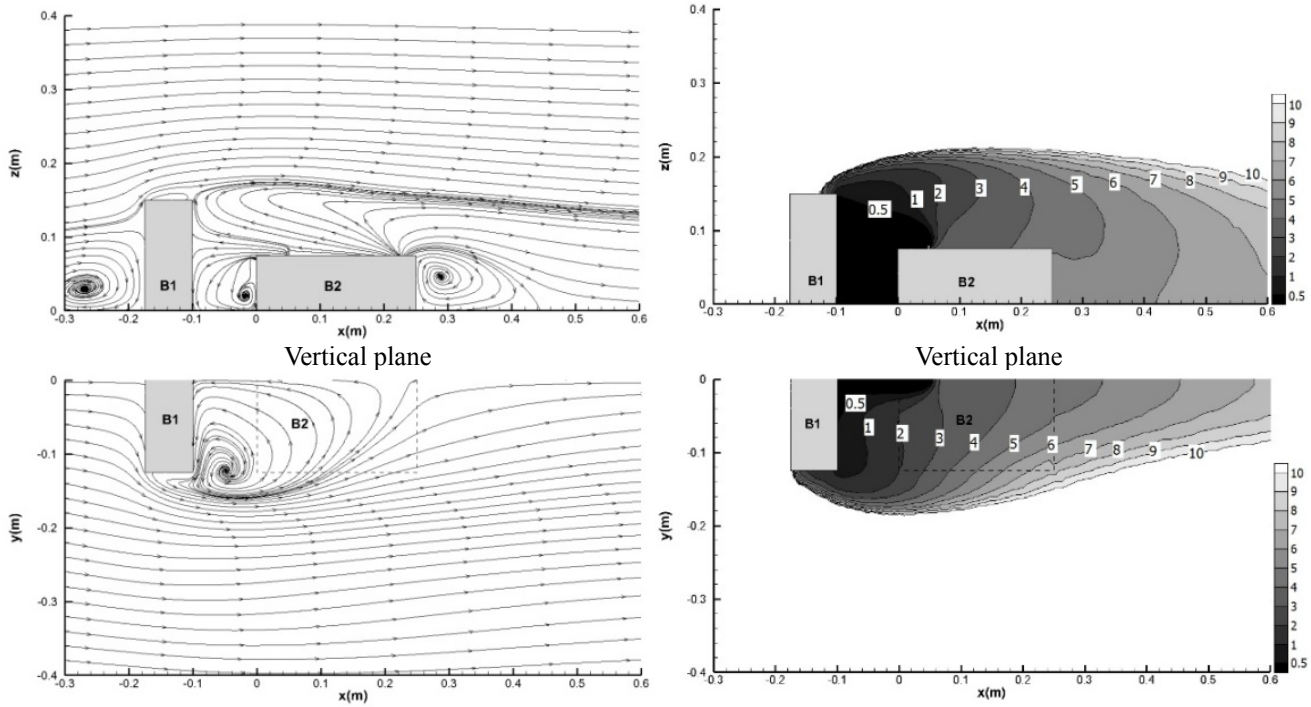

Vertical plane Vertical plane

Horizontal plane Horizontal plane

(a) Case 9 (H_{B1} = 0.15 m, X_s = 0.05 m)

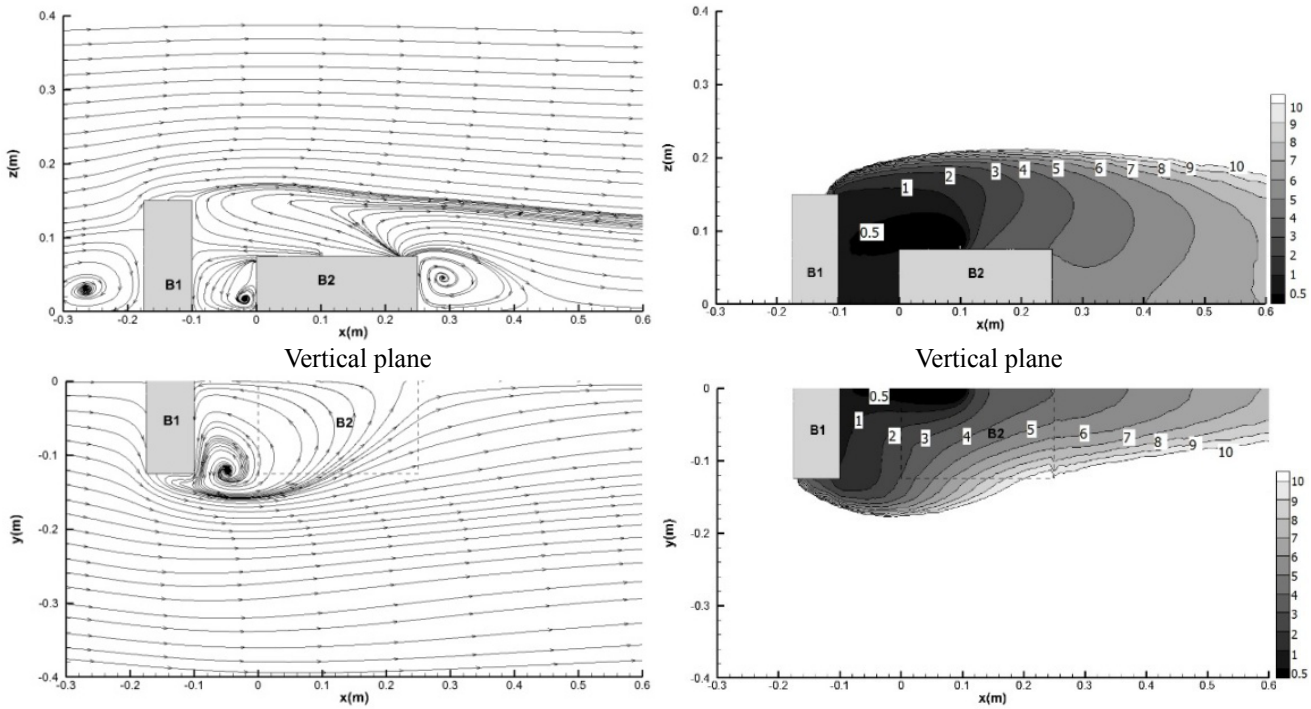

Vertical plane Vertical plane

Horizontal plane Horizontal plane

(b) Case 10 (H_{B1} = 0.15 m, X_s = 0.1 m)

Fig. 6. Streamlines and normalized dilution contours on the middle vertical plane and on the half horizontal plane at the stack height (z = 0.08 m) for the Cases 9–12 (H_{B1} = 0.15 m, X_s = 0.05, 0.1, 0.15, 0.2 m).

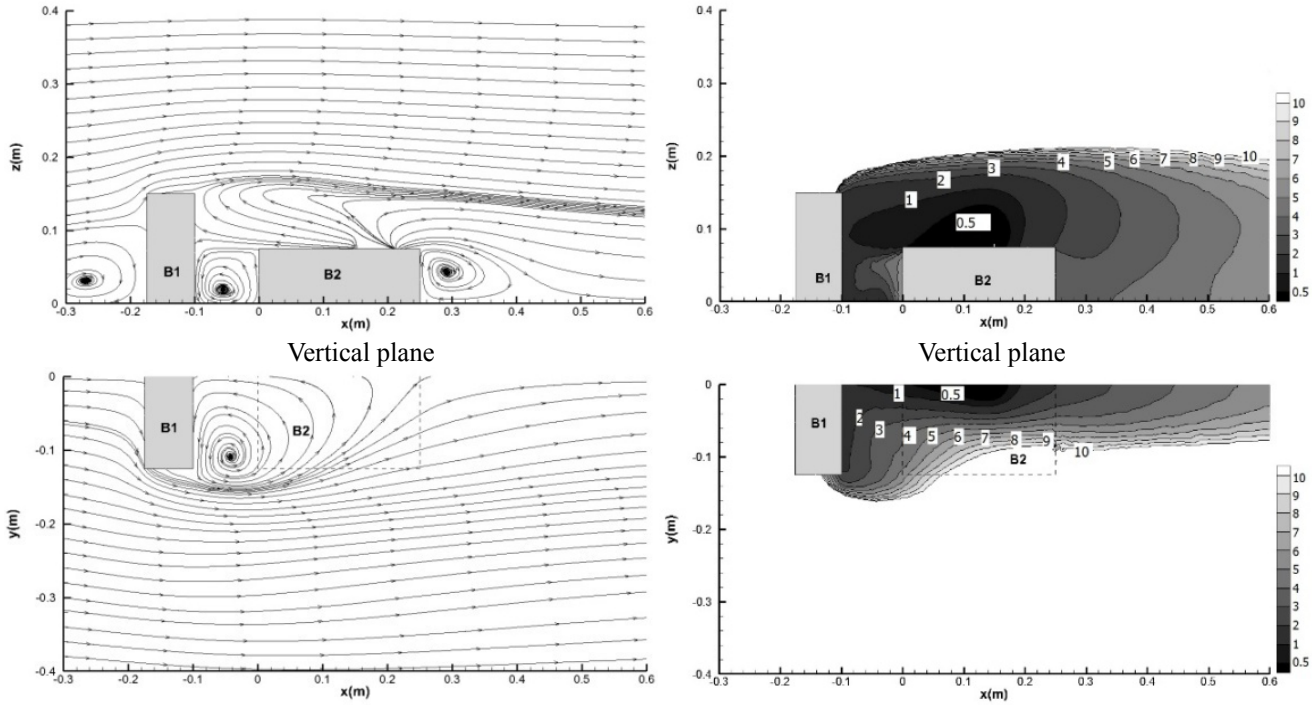

Vertical plane Vertical plane

Horizontal plane Horizontal plane

(c) Case 11 (H_{B1} = 0.15 m, X_s = 0.15 m)

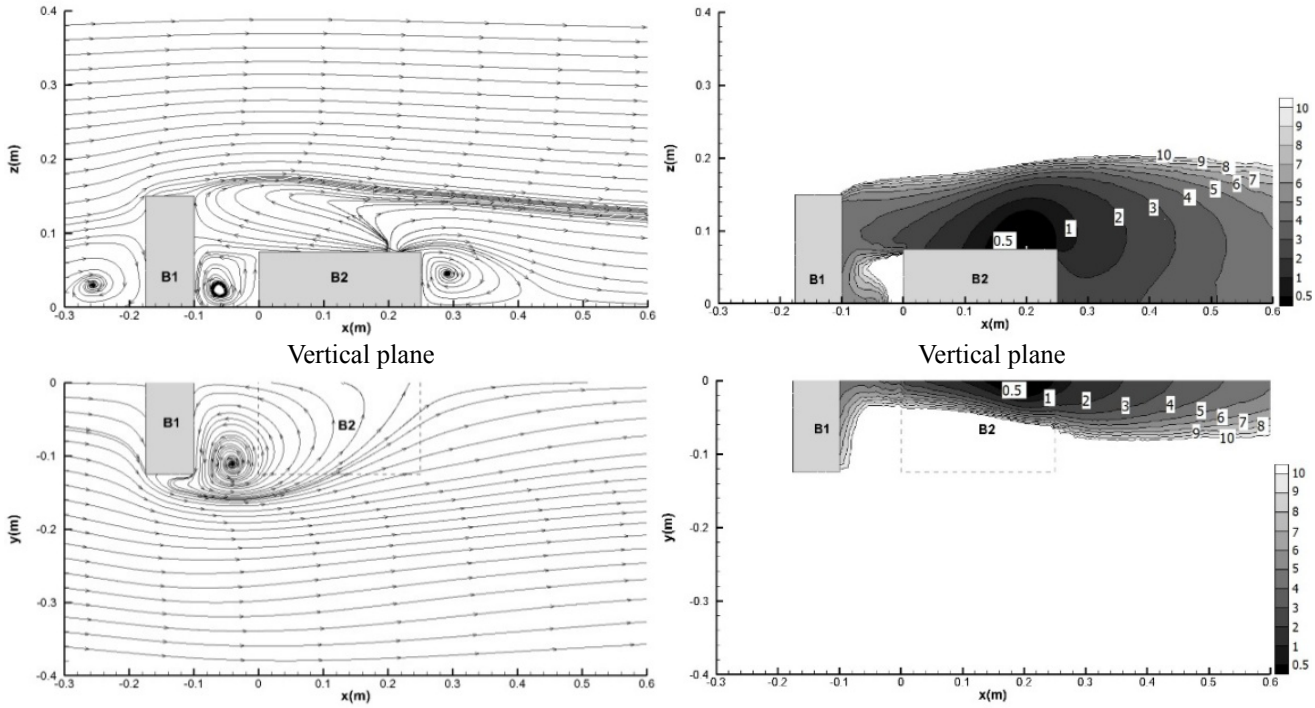

Vertical plane Vertical plane

Horizontal plane Horizontal plane

(d) Case 12 (H_{B1} = 0.15 m, X_s = 0.2 m)

Fig. 6. (*continued*).

emitting building increases with X_s. From Fig. 8, it can also be observed that the pollution level on the sidewall of the emitting building decreases with an increase of X_s (especially, pollutants are not detected on the sidewall of emitting building for the cases with X_s = 0.15 and 0.2 m). Furthermore, it can be seen from Fig. 8 that the pollutants are distributed on the sidewall of the upstream building for the cases with X_s = 0.05, 0.1 and 0.15 m.

Based on the pollutant distribution patterns on the middle vertical plane, on the horizontal plane at the stack

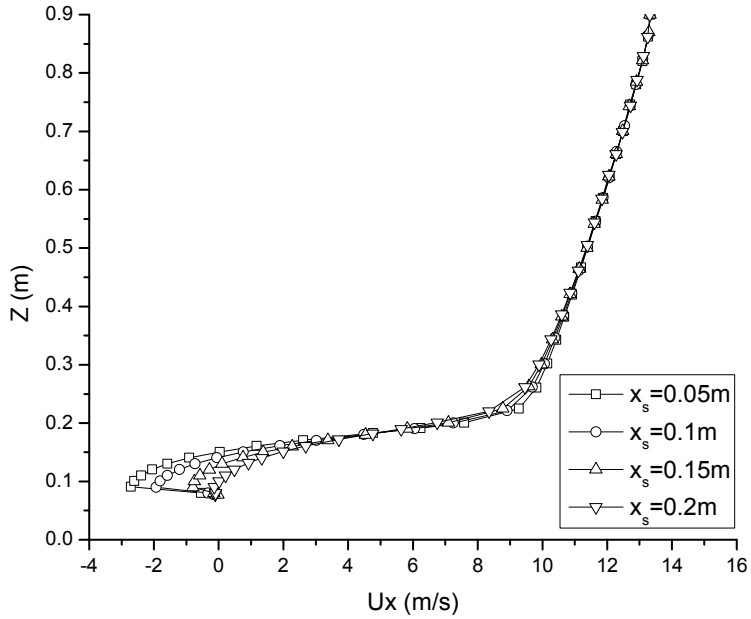

Fig. 7. Horizontal wind velocity component (U_x) profile along a vertical line above the stack for the Cases 9–12 (H_{B1} = 0.15 m, X_s = 0.05, 0.1, 0.15, 0.2 m).

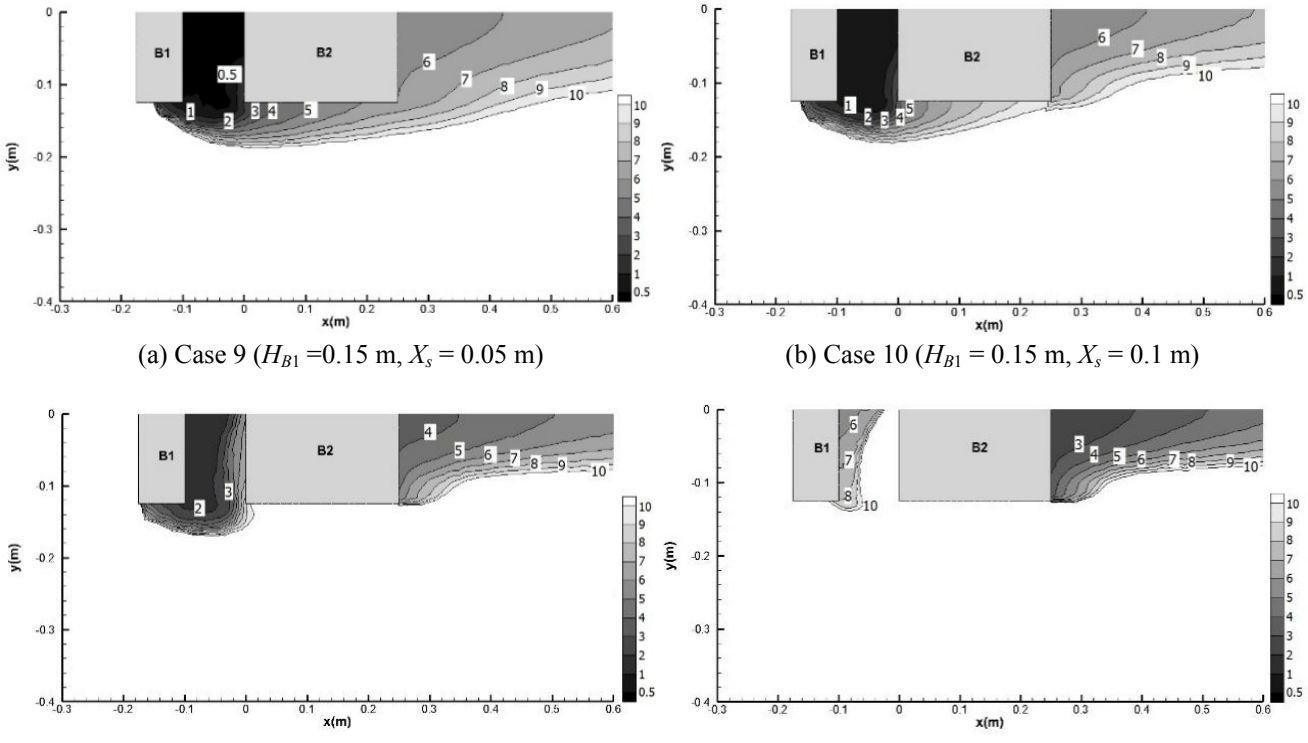

(a) Case 9 (H_{B1} =0.15 m, X_s = 0.05 m)

(b) Case 10 (H_{B1} = 0.15 m, X_s = 0.1 m)

(c) Case 11 (H_{B1} = 0.15 m, X_s = 0.15 m)

(d) Case 12 (H_{B1} = 0.15 m, X_s = 0.2 m)

Fig. 8. Distributions of normalized dilution at the height of 0.0075 m (1.5 m in full scale) above the ground floor for the Cases 9–12 (H_{B1} = 0.15 m, X_s = 0.05, 0.1, 0.15, 0.2 m).

height and on the horizontal plane at the human respiration height above the ground in the Cases 9–12, it can be revealed that: for the case with an upstream building of 0.15 m (H_{B1}/H_{B2} = 2.0) fresh air intakes should not be placed on the leeward wall of the upstream building, on the emitting building roof, or on the leeward wall of the emitting building as the stack is located within the recirculation zone of the upstream building; instead, they can be located on the windward wall of the upstream building and on the upwind part of the upstream building roof; additionally, whether or not an intake can be located on the sidewalls of the emitting building is dependent on the stack location (for example, a

fresh air intake can be placed on the lateral walls of the emitting building for X_s = 0.2 m but not on the lateral walls of the emitting building for X_s = 0.05 and 0.1 m).

Fig. 9 presents the streamlines and normalized dilution fields on the middle vertical plane and on the horizontal plane at the stack height for four various stack locations under an upstream building height of 0.27 m (H_{B1}/H_{B2} = 3.6). The streamlines on both the vertical and horizontal planes

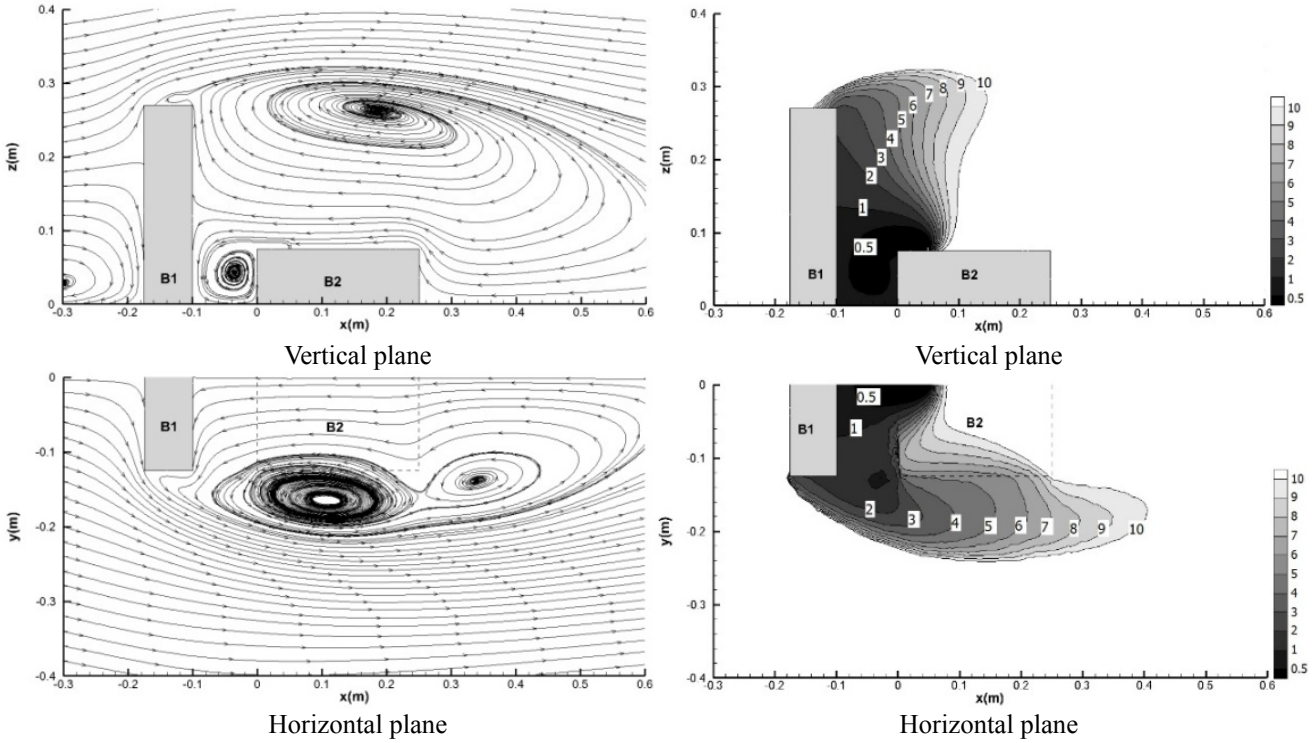

(a) Case 13 (H_{B1} = 0.27 m, X_s = 0.05 m)

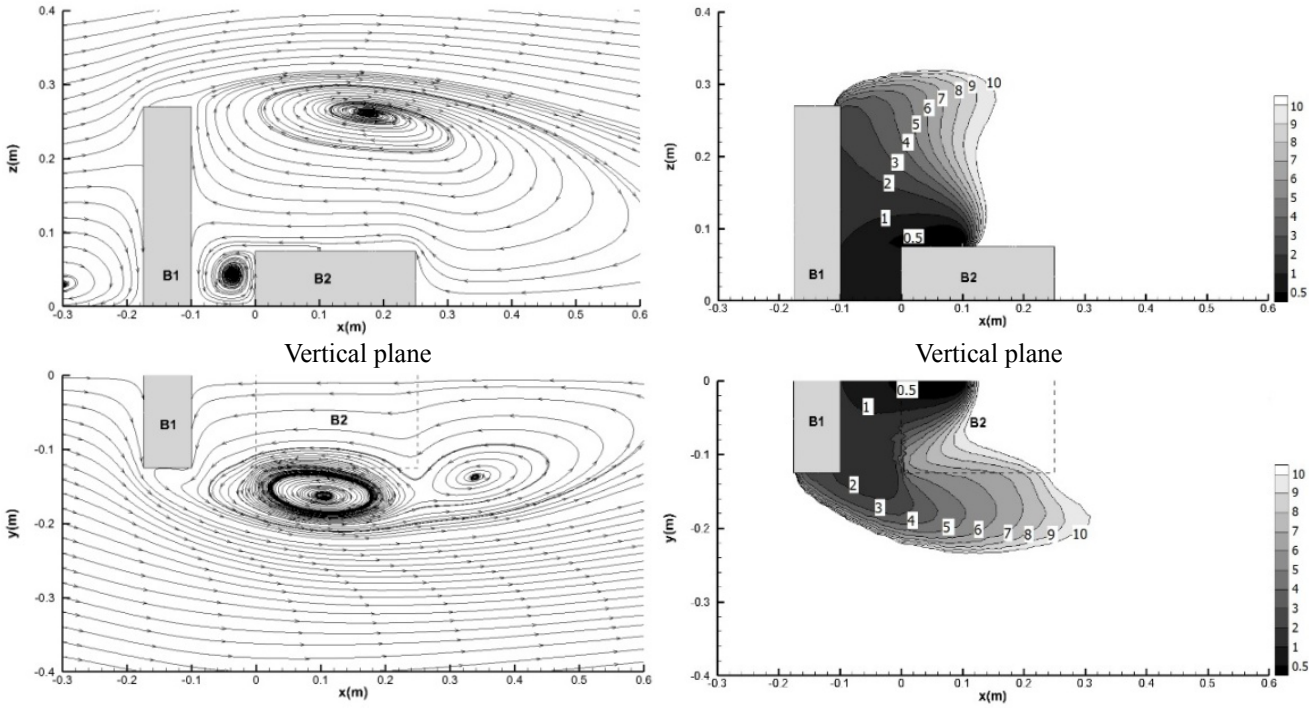

(b) Case 14 (H_{B1} = 0.27 m, X_s = 0.1 m)

Fig. 9. Streamlines and normalized dilution contours on the middle vertical plane and on the half horizontal plane at the stack height (z = 0.08 m) for the Cases 13–16 (H_{B1} = 0.27 m, X_s = 0.05, 0.1, 0.15, 0.2 m).

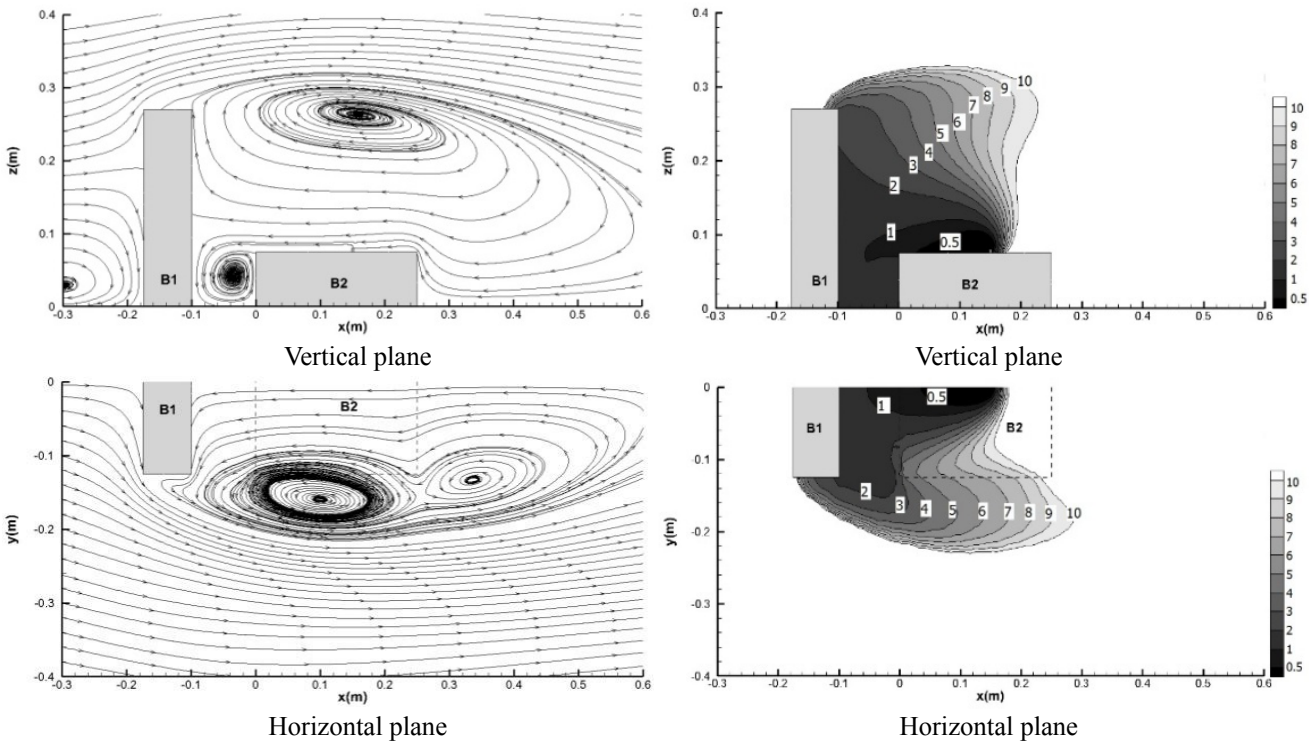

(c) Case 15 (H_{B1} = 0.27 m, X_s = 0.15 m)

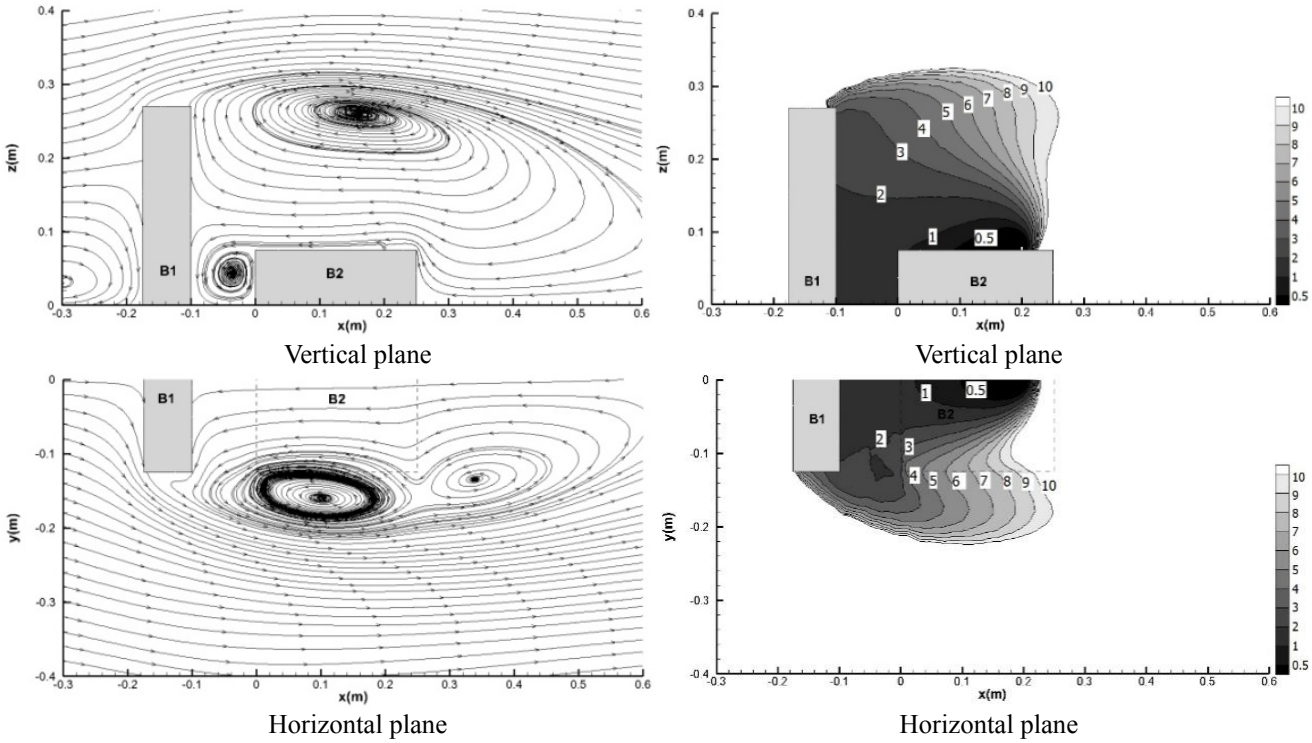

(d) Case 16 (H_{B1} = 0.27 m, X_s = 0.2 m)

Fig. 9. (*continued*).

reveal clearly that the general flow pattern is not influenced by the stack location under the condition of H_{B1} = 0.27 m. The streamlines on the vertical plane show clearly a huge clockwise vortex (i.e., the wake vortex of B1) with its center being located about the B1 height, a well-formed counter-clockwise vortex between the two buildings and a near-ground vortex next to the windward wall of B1. Clearly, the wake recirculation zone of B1 and the near-ground vortex next to the windward wall of B1 in the Cases 13–16 are substantially larger than those in the Cases 9–12 (see a

comparison of Fig. 6 with Fig. 9). Interestingly, the significant wake recirculation zones behind the emitting building found in the Cases 1–12 are not observed in the Cases 13–16 since the emitting building in the cases with H_{B1} = 0.27 m is fully immersed within the large wake recirculation zone behind the upstream building. The streamlines on the horizontal plane at the stack height in Fig. 9 show that a large horizontal vortex (yielding a cross flow) is formed inside the wake zone behind the upstream building (this horizontal vortex is greatly larger than that in the Cases 9–12).

Fig. 10 displays the distribution of horizontal wind velocity component (U_x) along the vertical line above the stack (the central point of the stack outlet is on this line) for the Cases 13–16. From Fig. 10, it is evident that for each of the Cases 13–16 the horizontal wind velocity component above the stack (up to almost the upstream building height) is directed upwind due to the large wake clockwise vortex of B1. Also, from Fig. 10, it can be observed clearly that the horizontal wind velocity component profile along the vertical line passing through the central point of stack outlet is almost unaffected by the stack location under the condition of H_{B1} = 0.27 m since the emitting building roof is fully located within the wake recirculation zone behind the upstream building. Comparing Fig. 10 with Fig. 7, it can be revealed clearly that for a given stack location (especially, for X_s = 0.1, 0.15 and 0.2 m) the upwind flow above the stack for the case with H_{B1} = 0.27 m is significantly stronger than that for the case with H_{B1} = 0.15 m.

For each of the Cases 13–16, the stack is located fully within the wake recirculation zone of the upstream building. The dilution contours on the middle vertical plane (see Fig. 9) show that a similar pollutant distribution pattern is produced for each of the Cases 13–16 (i.e., the pollutants are accumulated in the leeward side of the upstream building and in the canyon between the two buildings). This is because the entire plume released from the stack is trapped and swept towards the leeward side of the upstream building by the upwind flow which is nearly parallel to the roof surface of the emitting building. When the plume touches the leeward wall of the upstream building, a part of the pollutants are dragged by the anti-clockwise vortex into the canyon between the two buildings, whereas the other part of the pollutants are, at first, carried upwards by the upward wind and then dispersed downstream in the wake recirculation zone of the upstream building by the wake clockwise vortex. Furthermore, it can be observed from Fig. 9 that on the middle vertical plane the air pollution area tends to expand with an increase of X_s whereas the pollution levels along the leeward wall of upstream building and inside the canyon between the two buildings decrease with an increase of X_s. The dilution contours on the horizontal plane also reveal that a similar pollutant distribution pattern is formed on the horizontal plane at the stack height for each of the Cases 13–16: a portion of the pollutants carried by the upwind flow are caught and then transported transversally by the large horizontal vortex (cross flow) resulting in significant air pollution inside the canyon between the two buildings, on the roof of emitting building and near the sidewalls of the two buildings. Clearly, the polluted region on the emitting building roof increases with X_s under the condition of H_{B1} = 0.27 m.

Fig. 11 shows the distributions of the normalized dilution contours at the height of 0.075m (corresponding to 1.5m in full scale) above the ground floor for the Cases 13–16. From Fig. 11, it can be seen clearly that for each of the Cases 13–16 high pollution level is formed in the region between the two buildings and significant pollutant distributions are observed on the sidewalls of the two buildings. Also, the region behind the emitting building is almost free of pollutants for each of the Cases 13–16.

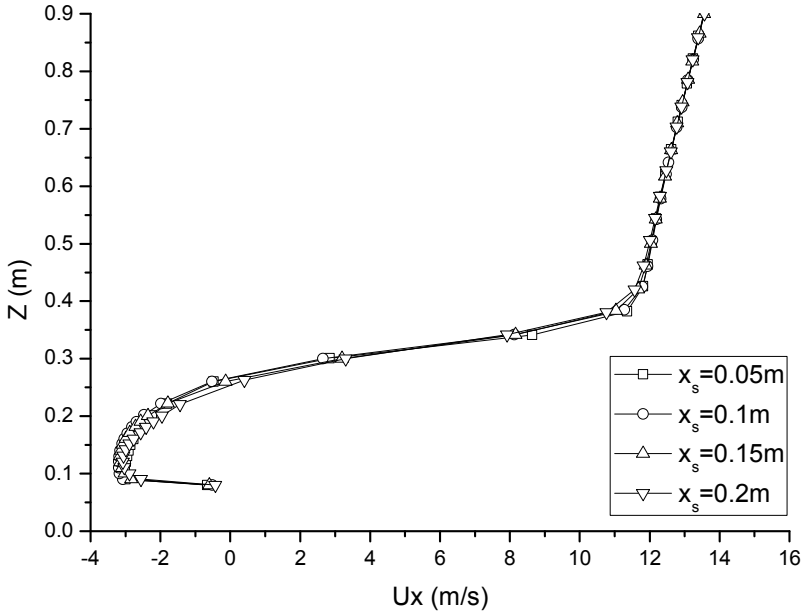

Fig. 10. Horizontal wind velocity component (U_x) profile along a vertical line above the stack for the Cases 13–16 (H_{B1} = 0.15 m, X_s = 0.05, 0.1, 0.15, 0.2 m).

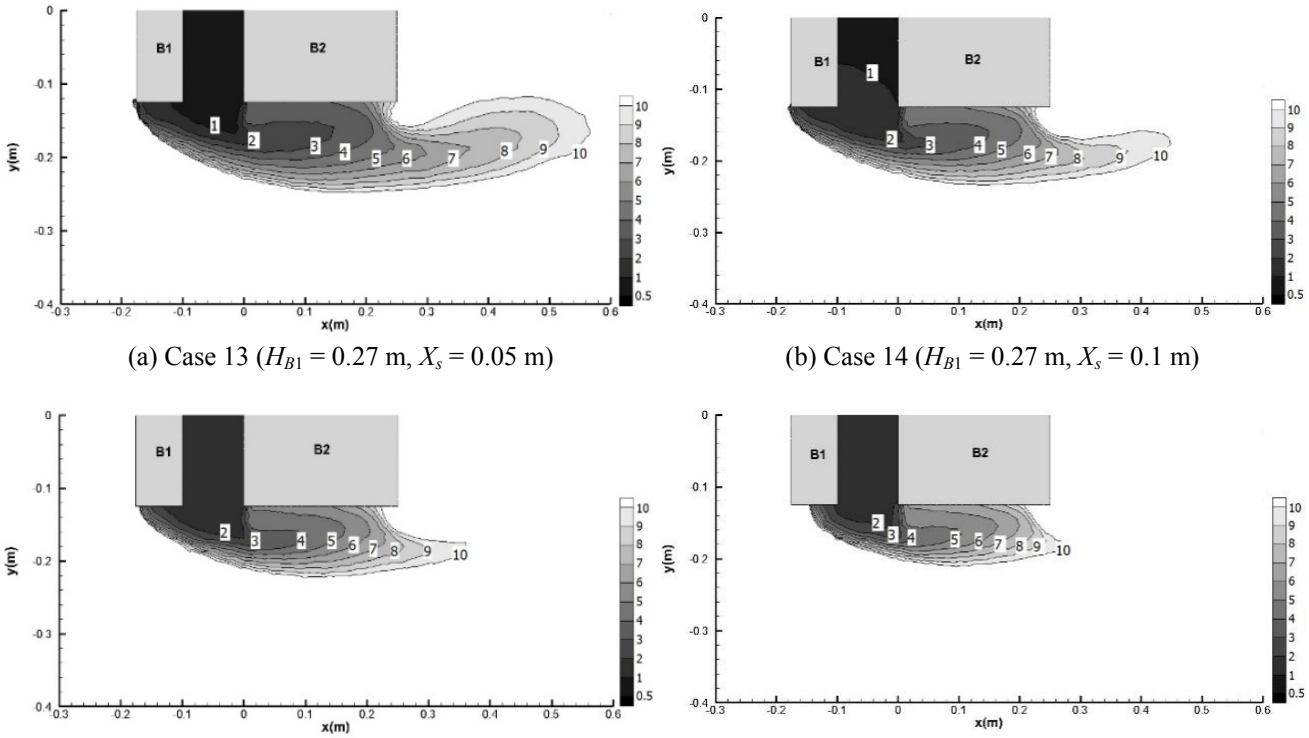

(a) Case 13 (H_{B1} = 0.27 m, X_s = 0.05 m) (b) Case 14 (H_{B1} = 0.27 m, X_s = 0.1 m)

(c) Case 15 (H_{B1} = 0.27 m, X_s = 0.15 m) (d) Case 16 (H_{B1} = 0.27 m, X_s = 0.2 m)

Fig. 11. Distributions of normalized dilution at the height of 0.0075 m (1.5 m in full scale) above the ground floor for the Cases 13–16 (H_{B1} = 0.27 m, X_s =0.05, 0.1, 0.15, 0.2 m).

Based on the pollutant distribution patterns on the middle vertical plane, on the horizontal plane at the stack height and on the horizontal plane at the human respiration height above the ground in the Cases 13–16, it can be revealed that for the case with an upstream building of 0.27 m (H_{B1}/H_{B2} = 3.6) fresh air intakes should not be placed on the emitting building roof upwind the stack, on the lateral and windward walls of the emitting building, or on the leeward and lateral walls of the upstream building (instead, intakes can be located on the leeward wall of the emitting building, on the emitting building roof downwind the stack, on the windward wall of the upstream building and on the upstream part of the upstream building roof).

Chavez *et al.* (2012) also performed a CFD study on flow and pollutant dispersion in the above Cases 10 and 14. It is worth pointing out here that the numerical results in the current study are almost exactly the same as those obtained by Chavez *et al.* (2012) in their CFD simulations in terms of the streamlines and dilution contours on the middle vertical plane and on the horizontal plane at the stack height for the Cases 10 and 14.

SUMMARY AND CONCLUSIONS

This paper presents 3D CFD simulations to study the effects of the upstream building height and stack location on the pollutant dispersion from a rooftop stack in an urban environment. The simulations are performed using the steady RANS equations coupled with Realizable k-ε turbulence model and the species transport equation for passive and inert pollutant concentration. In the CFD modeling, the approaching wind is orthogonal to the building faces and the gaseous pollutants (SF_6) are released continuously from a rooftop stack. The flow development and pollutant dispersion are investigated numerically considering the combinations of four different upstream building heights with four different stack locations (therefore, sixteen cases are adopted depending on the various combinations of upstream building height and stack location). The numerical results reveal clearly that the dilution of the pollutants emitted from a rooftop stack is affected significantly by the upstream building height and stack location. The main conclusions of this paper can be summarized for each case, as follows:

Upstream Building of Lower or Equal Height with the Emitting Building

(1) On the middle vertical plane passing through the center of the stack outlet, as the upstream building height increases from $0.5H_{B2}$ to H_{B2} both the near-ground vortex next to the windward wall of the upstream building and the vortex inside the canyon enclosed by the two buildings enlarge greatly while the wake vortex behind the emitting building diminishes significantly. The cross flow is not established on the horizontal plane at the stack height. Irrespective of the stack location, the stack effluents are immediately transported downwind the stack by the longitudinal wind.

(2) Fresh air intakes should not be placed on the emitting building roof downwind the stack or on the leeward wall of the emitting building. Instead, they can be located

on the whole upstream building surfaces, on the lateral and windward walls of the emitting building, and on the emitting building roof upwind the stack.

Upstream Building Higher than the Emitting Building

(1) When the emitting building is partly located within the wake vortex zone behind the upstream building (e.g., the cases with H_{B1}/H_{B2} = 2.0), a combination of upwind and downwind flows above the emitting building roof as well as three vortices (i.e., a near-ground vortex next to the windward wall of the upstream building, an anti-clockwise vortex in the canyon and a wake vortex behind the emitting building) are formed on the middle vertical plane and a cross flow is established on the horizontal plane at the stack height. When the emitting building is located fully within the wake vortex zone of the upstream building (e.g., the cases with H_{B1}/H_{B2} = 3.6), a huge clockwise vortex (i.e., the wake vortex of the upstream building) with its center being located about the upstream building height, a well-organized counter-clockwise vortex within the canyon and a near-ground vortex next to the windward wall of the upstream building are developed on the middle vertical plane and a strong cross flow is set up on the horizontal plane at the stack height. On the middle vertical plane the wake vortex zone behind the upstream building for the cases with H_{B1}/H_{B2} = 3.6 is substantially larger than that for the cases with H_{B1}/H_{B2} = 2.0. Also, on the horizontal plane at the stack height the cross flow for the cases with H_{B1}/H_{B2} = 3.6 is significantly stronger than that for the cases with H_{B1}/H_{B2} = 2.0. For the cases with H_{B1}/H_{B2} = 2.0, the pollutants emitted from the stack located in the wake vortex zone of the upstream building are dragged by the upwind flow towards the upstream building, yielding the following results: (a) a part of the pollutants carried by the upwind flow are trapped by the in-canyon vortex, resulting in pollutant pileup inside the canyon; (b) as the pollutants reach the leeward side of the upstream building, they are conveyed downstream by the downwind flow, thus leading to a long zone of contamination; (c) a significant pollutant distribution along the building width direction is formed on the horizontal plane at the stack height because a part of the pollutants carried by the upwind flow are transported transversally by the cross flow; (d) the pollution levels inside the canyon and on the leeward wall of the upstream building as well as the polluted area on the horizontal plane at the stack height decrease with an increase of the distance between the stack and the upwind edge of emitting building. For each of the cases with H_{B1}/H_{B2} = 3.6, the entire plume released from a stack is trapped and swept towards the leeward side of the upstream building by the huge clockwise vortex, yielding the following results: (a) as the plume touches the leeward wall of the upstream building some part of the pollutants are dragged into the canyon by the in-canyon vortex whereas the other part of the pollutants are, at first, carried upwards by the upward wind and then dispersed downstream in the wake zone behind the upstream building; (b) on the middle vertical plane, as the distance between the stack and the upwind edge of the emitting building increases the polluted area expands while the pollution levels on the leeward wall of the upstream building and inside the canyon decrease; (c) on the horizontal plane at the stack height, a portion of the pollutants carried by the huge clockwise vortex are conveyed transversally by the large horizontal vortex, resulting in significant pollution inside the canyon, on the emitting building roof and near the sidewalls of the two buildings; (d) the polluted region on the emitting building roof increases as the stack moves closer to the downwind edge of the emitting building.

(2) For an emitting building located partly within the wake zone behind the upstream building, as the stack is located within the wake zone behind the upstream building, fresh air intakes should not be placed on the leeward wall of the upstream building, on the emitting building roof or on the leeward wall of the emitting building (instead, intakes may be located on the windward wall of the upstream building and on the upwind part of the upstream building roof). For an emitting building located fully within the wake vortex zone of the upstream building, regardless of the stack location, fresh air intakes should not be placed on the emitting building roof upwind the stack, on the lateral and windward walls of the emitting building, or on the leeward and lateral walls of the upstream building (instead, intakes can be located on the leeward wall of the emitting building, on the windward wall of the upstream building and on the upwind part of the upstream building roof).

ACKNOWLEDGEMENTS

This work was supported by the National Natural Science Foundation of China (Grant No. 51536006).

REFERENCES

Chavez, M., Hajra, B., Stathopoulous, T. and Bahloul, A. (2011). Near-field pollutant dispersion in the built environment by CFD and wind tunnel simulations. *J. Wind Eng. Ind. Aerodyn.* 99: 330–339.

Chavez, M., Hajra, B., Stathopoulous, T. and Bahloul, A. (2012). Assessment of near-field pollutant dispersion: Effect of upstream buildings. *J. Wind Eng. Ind. Aerodyn.* 104: 509–515.

Gupta, A., Stathopoulous, T. and Saathoff, P. (2012). Wind tunnel investigation of the downwash effect of a rooftop structure on plume dispersion. *Atmos. Environ.* 46: 496–507.

Hajra, B., Stathopoulous, T. and Bahloul, A. (2011). The effect of upstream buildings on near-field pollutant dispersion in the built environment. *Atmos. Environ.* 45: 4930–4940.

Hajra, B. and Stathopoulous, T. (2012). A wind tunnel study of the effect of downstream buildings on near-field

pollutant dispersion. *Build. Environ.* 52: 19–31.

Huang, Y.D., Long, C., Deng, J.T. and Kim, C.N. (2014). Impacts of upstream building width and upwind building arrangements on airflow and pollutant dispersion in a street canyon. *Environ. Forensics* 15: 25–36.

Li, X.X., Liu, C.H., Leung, D.Y.C. and Lam, K.M. (2006). Recent progress in CFD modelling of wind field and pollutant transport in street canyons. *Atmos. Environ.* 40: 5640–5658.

Ramponi, R. and Blocken, B. (2012). CFD simulation of cross-ventilation for a generic isolated building: Impact of computational parameters. *Build. Environ.* 53: 34–48.

Tominaga, Y. and Stathopoulous, T. (2009). Numerical simulation of dispersion around an isolated cubic building: Comparison of various types of *k*-ε models. *Atmos. Environ.* 43: 3200–3210.

Wilson, D.J., Fabris, I., Chen, J., Ackerman, M. (1998). Adjacent building effects on laboratory fume hood exhaust stack design. ASHRAE Research Report 897, American Society of Heating and Refrigerating and Air-conditioning Engineers, Atlanta, USA.

Yassin, M.F. (2013). Experimental study on contamination of building exhaust emissions in urban environment under changes of stack locations and atmospheric stability. *Energy Build.* 62: 68–77.

Received for review, May 16, 2016
Revised, December 8, 2016
Accepted, March 2, 2017